The Law of Absolute Gravity

George Park
November 3, 2019
2019 Science Symposium II
Urantia Foundation, Chicago, Illinois

In the cosmology of *The Urantia Book* everything revolves around the center of the universe. Universal revolution is explained by a new law of gravity called absolute or Paradise gravity. This revolving model is radically different from the current model of an expanding universe. This standard model is explained by linear gravity, as described in the theory of general relativity. It is assumed here the revolving model is destined to supersede the expanding model. The transition to this new cosmological paradigm will require, among other things, very substantial evidence that absolute gravity is real.

This paper attempts to take a step in this direction. It approaches absolute gravity as a scientific hypothesis which can explain certain facts discovered by observational astronomy. Part I reviews the revolving model and identifies two cosmic structures described in it. Part II identifies the properties of absolute gravity and the central force with these properties. An equation for cosmological redshift is derived from special relativity, and the hypothesis is subjected to a critical test. The conclusion reached is that the theory of absolute gravity is scientifically superior to linear gravity on large cosmic scales, because it has greater predictive and explanatory power. The revolving model has an elegant simplicity which surpasses the arcane complexity of the expanding model.

PART I: The Revolving Model of the Universe

1. Space Levels of the Master Universe

I. The Six Concentric Space Levels

(*Not Drawn to Scale*)

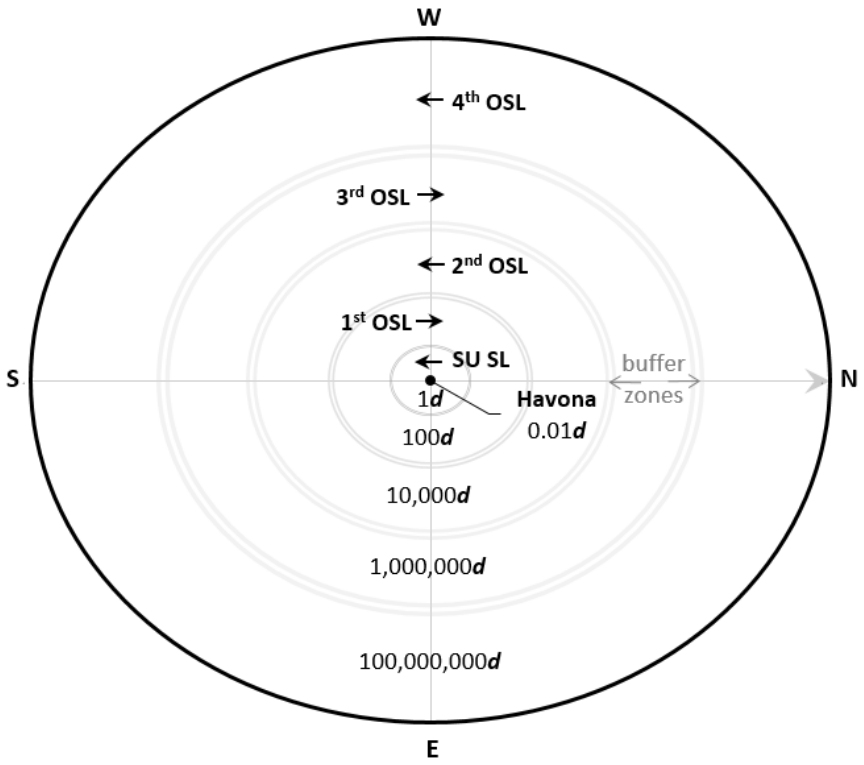

In the book's model the universe revolves around Paradise in response to absolute gravity (I). Universal revolution results in a gravitational "plane of creation." [11:7.6] The vertical height and depth from this horizontal plane increases as the distance from Paradise increases. [11:7.6] This plane consists of six concentrically arranged space levels [11:8.2] with the elliptical form of Paradise. [15:4.1] [11:2.2] These six space levels constitute the master universe. The smallest space level is the central universe of Havona, which is surrounded by the superuniverse space level (SU SL). Encircling the superuniverse space level are the first through fourth outer space levels (1st – 4th OSL).

The space levels revolve in alternating directions. [11:7.9] The opposite directions of motion between neighboring space levels require intervening buffer zones. "These zones separate the vast galaxies which race around Paradise in orderly procession." [11:7.7] The buffer zone between the superuniverse and first outer space levels is half a million light-years wide. [12:1.14] The one between the first and second outer space levels is 50 million

light-years, or 100 times wider. [12:1.15] This implies the widths of successive space levels also increase by a scale factor of 100. The first outer space level is 100 times wider than the superuniverse space level, which is 100 times wider than Havona.

II. Internal Structure of the Superuniverse Space Level

(Drawn to Scale)

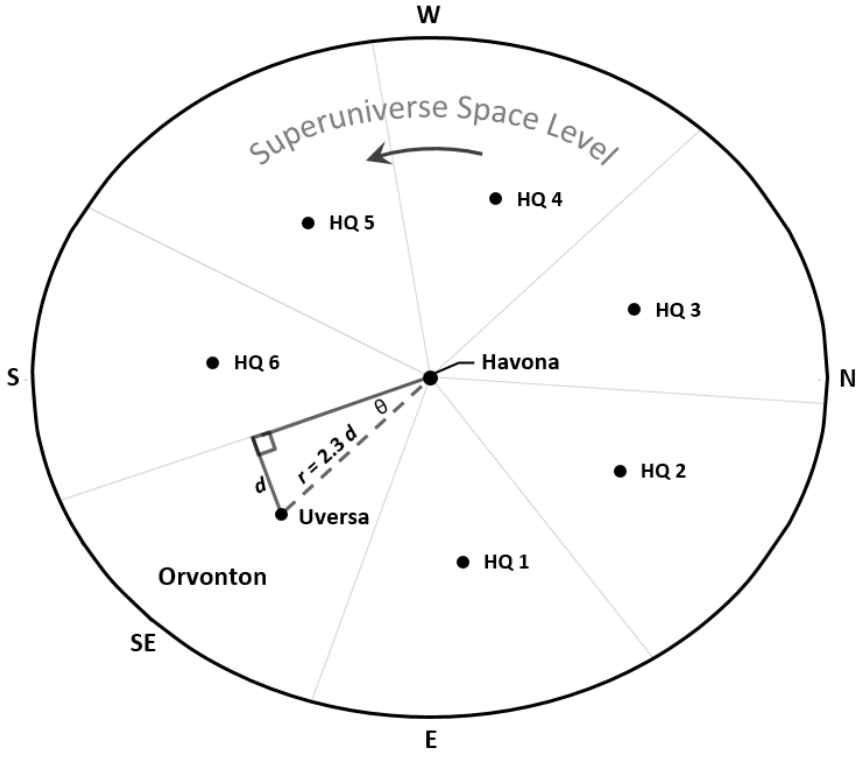

The Milky Way is located in the superuniverse space level (II). This space level is equally partitioned in seven wedge-like segments. Each of these seven space segments contains a superuniverse with its galaxies ("many island universes" [12:2.3]). These seven segments are separated by "radial boundary lines" which converge at Paradise. [16:0.12] The first thing created in each superuniverse is its headquarters world. [15:0.2] The headquarters world in our superuniverse of Orvonton is called Uversa, which is located southeast of the Isle of Paradise. [15:1.5]

Each headquarters world is located in the center of its space segment. [15:7.1] Uversa is halfway between Paradise and the outer border of Orvonton and halfway between its two radial boundary lines. These boundary lines are separated by 51.4° of arc (360°/7). Since Uversa is located halfway between these boundaries, a line drawn from Uversa to Paradise and up along a radial boundary line forms an angle of 25.7°. From the sine of this angle, the distance r from Uversa to Paradise is 2.3 times the shortest distance d from Uversa to Orvonton's radial boundary ($r = d/\sin 25.7° = 2.3d$).

III. The Ring of Galaxies in the Superuniverse Space Level

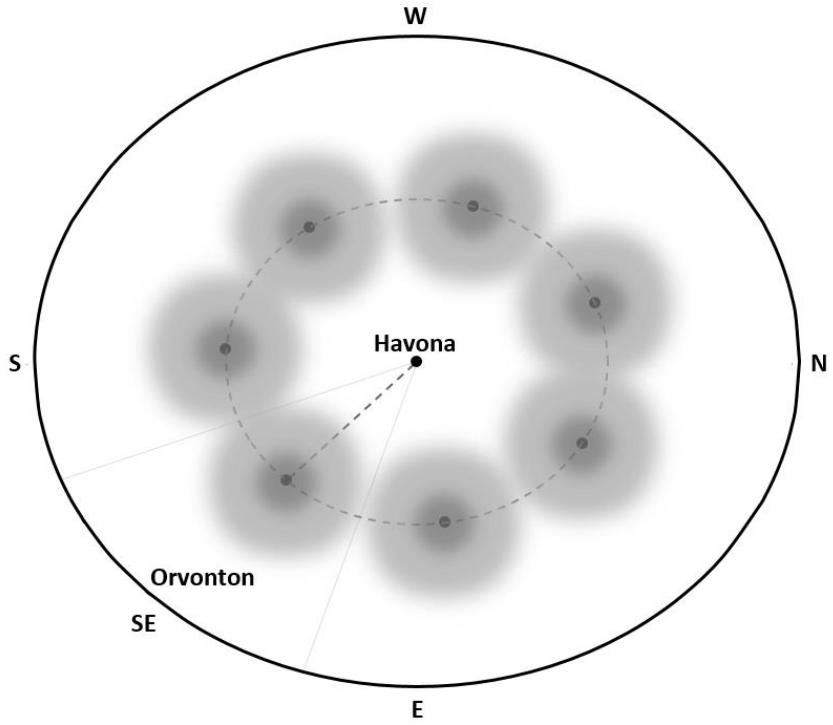

The many galaxies in each superuniverse revolve around its headquarters world. 15:3.7 15:3.13 Gravitational revolution requires a concentration of matter in the center of a system, such as occurs in the galactic bulge at the center of the Milky Way. Galaxies in a superuniverse should cluster in the region of its headquarters world. The circular arrangement of headquarters worlds forms a ring-like concentration of seven galactic clusters.

IV. The Central Core and Kernel

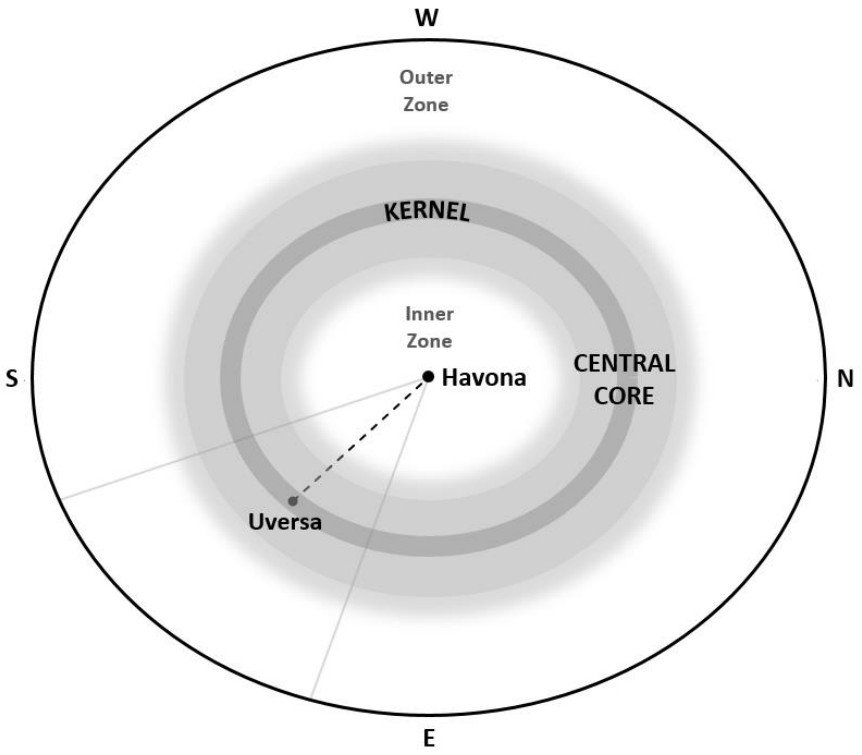

This ring of galaxies (IV) can be called the central core of the space level. The density of galaxies in the superuniverse space level is highest in the central core. The density of galaxies within the central core is highest in the middle of the central core. This circle of maximum galactic density can be called the kernel.

V. Galactic Densities by Horizontal Distance from Paradise and Vertical Distance from the Plane of Creation

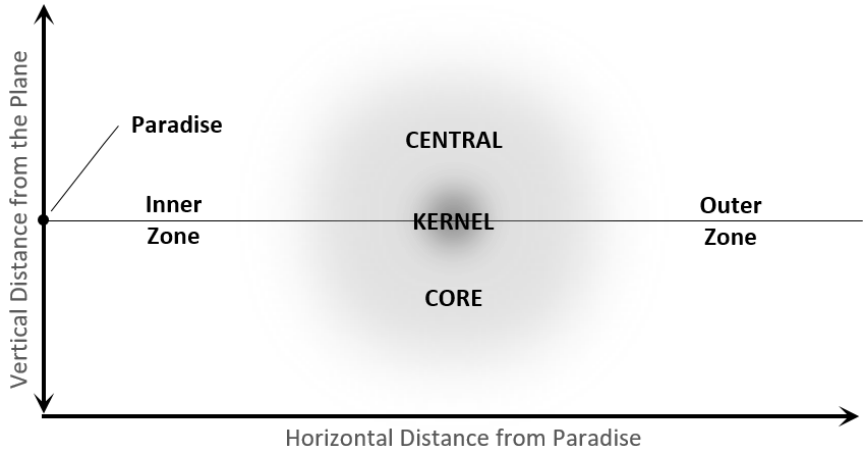

Galactic densities in the superuniverse space level can be considered in two dimensions. The horizontal distances of galaxies from Paradise can be plotted against

their vertical distances above or below the plane of creation (V). The maximum galactic density occurs in the kernel, which is on this plane. The density should decrease moving away from the kernel in both the horizontal and vertical directions.

This scalable model describes a ring-like central core in the middle of the superuniverse space level. Uversa is located in the kernel at the heart of this central core. The distance from Uversa to Paradise is 2.3 times the shortest distance from Uversa to the radial boundary lines of Orvonton. This shortest distance equals the radius of Orvonton in a direction that is roughly perpendicular to Paradise.

2. The Galaxies of Orvonton

VI. The Local Group in the Central Portion of Orvonton

Polar view of the equatorial plane

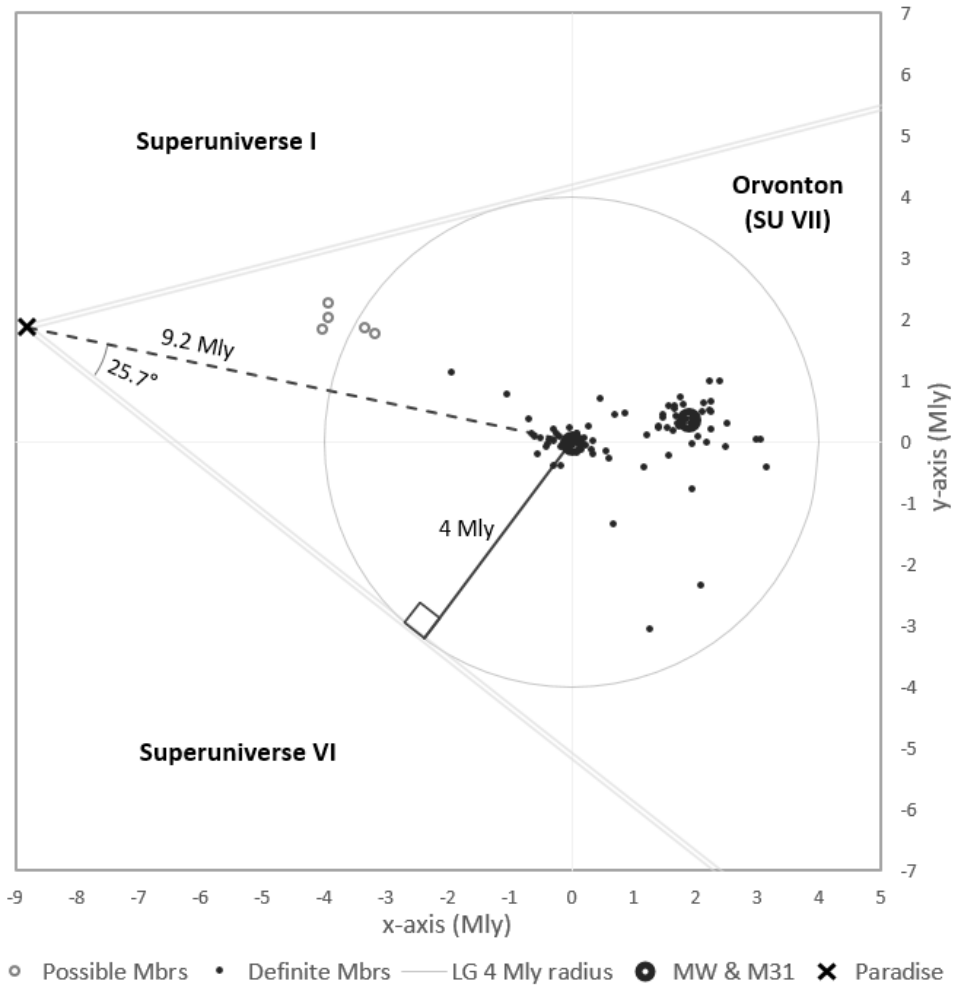

This conceptual model needs two facts to become a concrete model; the distance to Uversa and the shortest distance to the radial boundary lines of Orvonton. The book gives a distance of about 200,000 light-years to Uversa. 32:2.11 This is relatively nearby, since the Milky Way has a radius of 50,000 light-years. The Milky Way is part of a collection of galaxies called the Local Group, first identified in 1936. [1] These galaxies are bound together by gravity and move as a single unit. [2] The Local Group contains 99 definite member galaxies, as of 2019. [See Appendix] This is consistent with the statement that there are "many island universes" in Orvonton. 12:2.3

The Local Group occupies the central portion of Orvonton (VI), since "The vast Milky Way starry system represents the central nucleus of Orvonton." 15:3.1 A radius of about 4 million light-years (Mly) (± 550,000 light-years) encompasses the Local Group. The shortest distance from Uversa to the radial boundaries of Orvonton is assumed to be 4 Mly. The distance from Uversa to Paradise is 2.3 times this or 9.2 Mly. The distance to the far border of the superuniverse space level is three times this or 27.6 Mly. This is within a region of galactic over-density referred to as the Local Volume, which extends out to 32 Mly (10 Mpc). The central core should be within the Local Volume.

The Milky Way appears as a belt of stars, because our sun is on its gravitational plane. Uversa is on the plane of creation and we are near Uversa. From this perspective the central core should appear as a belt of galaxies on the celestial sphere.

VII. The 122 Galaxies known to be within the Local Volume in 1956

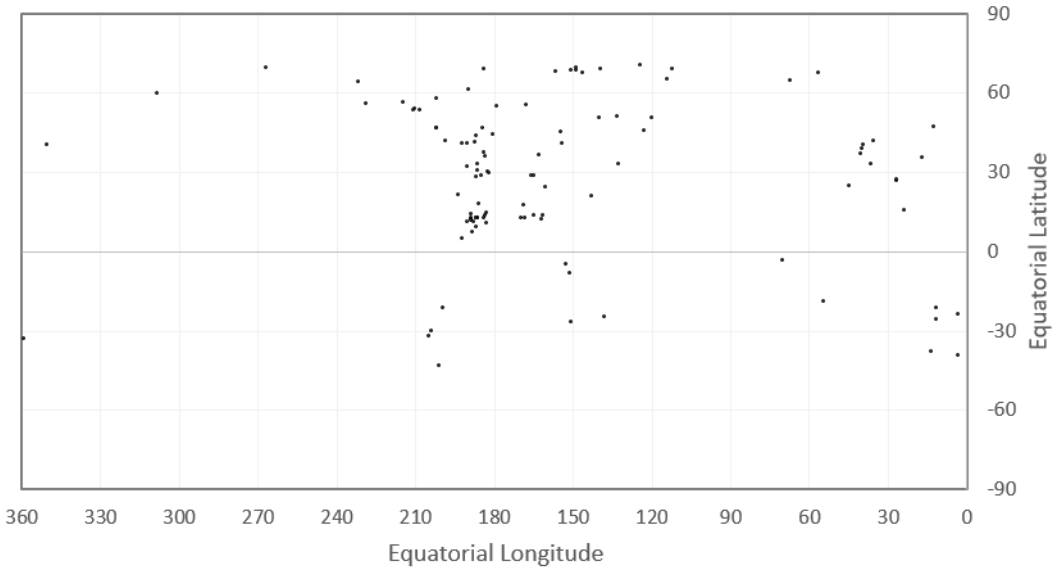

Nothing like this was observable in 1955. A comprehensive list of 812 galaxies with measured redshifts was published in 1956. [3] Only 122 galaxies have redshifts which

place them within the Local Volume. Plotting them on an all-sky map (VII) does not show anything like a belt of galaxies.

3. The Kernel and Central Core of the Superuniverse Space Level

The number of galactic redshift measurements has increased dramatically and are catalogued in NASA's Extragalactic Database. [4] Distances for galaxies beyond the Local Group can be calculated from their redshifts. A 2018 query of this database for all galaxies with good redshift measurements (i.e. no redshift flags) placing them between 5 and 32 Mly away produces a list of 5,162 galaxies.

VIII. All-Sky Map of 5,162 Galaxies within 5-32 Million Light-Years

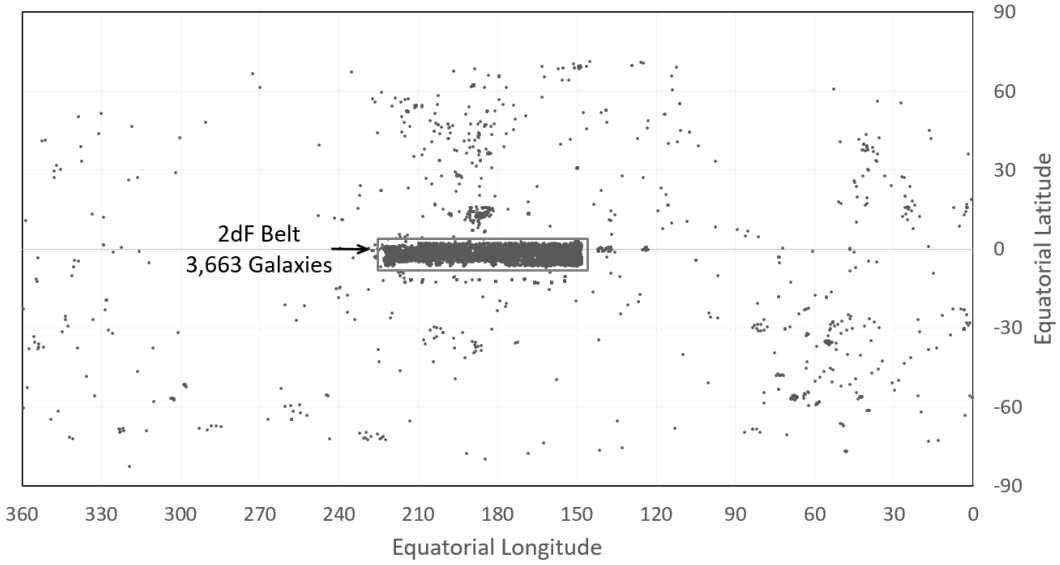

IX. 3,663 Galaxies within the 2dF Survey Window

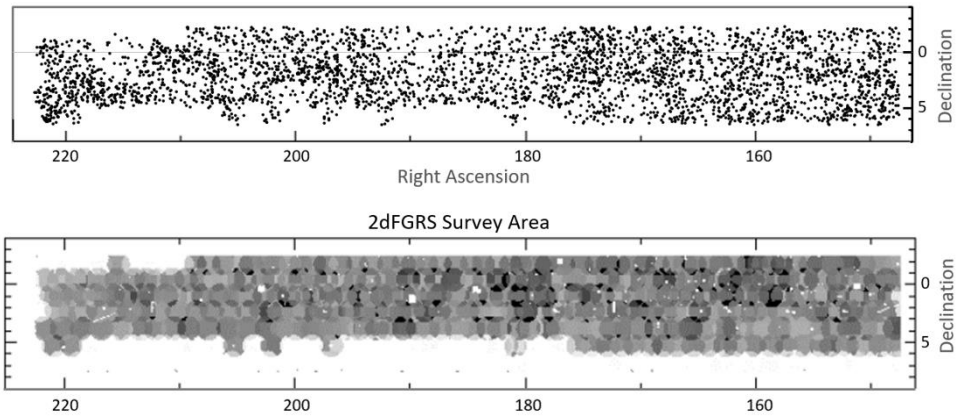

Plotting these galaxies on an all-sky map (VIII) shows a continuous belt of 3,964 galaxies along the celestial equator that is 75° of longitude in length and about 9° of

latitude in height. The outline of this belt is an artifact of the survey design for the automated 2-degree-Field Galactic Redshift Survey (IX). The overwhelming majority of the galaxies in this belt, or 3,663 galaxies, come from this 2dF survey. Mapping the 2dF belt of galaxies in three-dimensions shows an orderly arrangement.

X. Polar View of the 3,663 Galaxies in the 2dF Belt

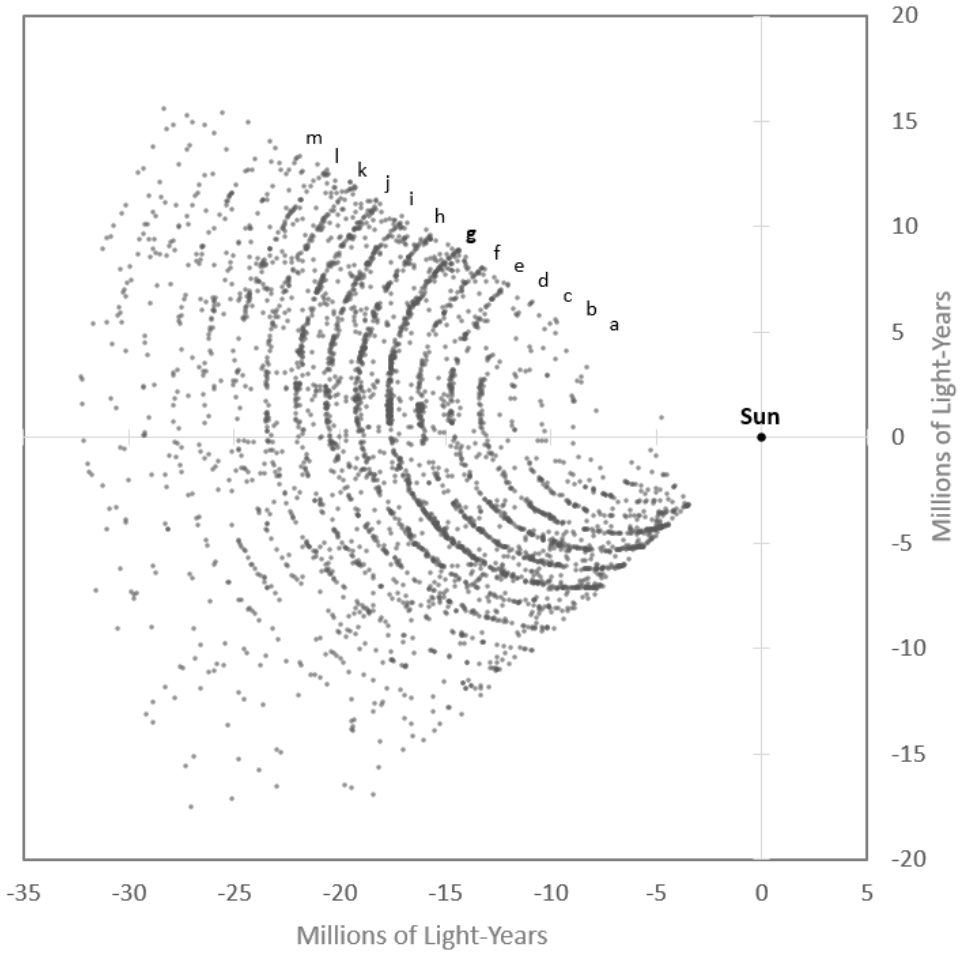

Looking down on the celestial plane from the North Pole (X), the 2dF belt of galaxies is arranged in concentric arcs separated by 1.25 Mly. This spacing is due to technical limitations in measuring redshifts (typical accuracy is about one ten-thousandth the speed of light.) For convenience of reference, these arcs are labeled *a* through *m.* The kernel should be the arc of galaxies with the highest galactic density.

XI. Density of Galaxies in Arcs *a* through *m* in the 2dF Belt

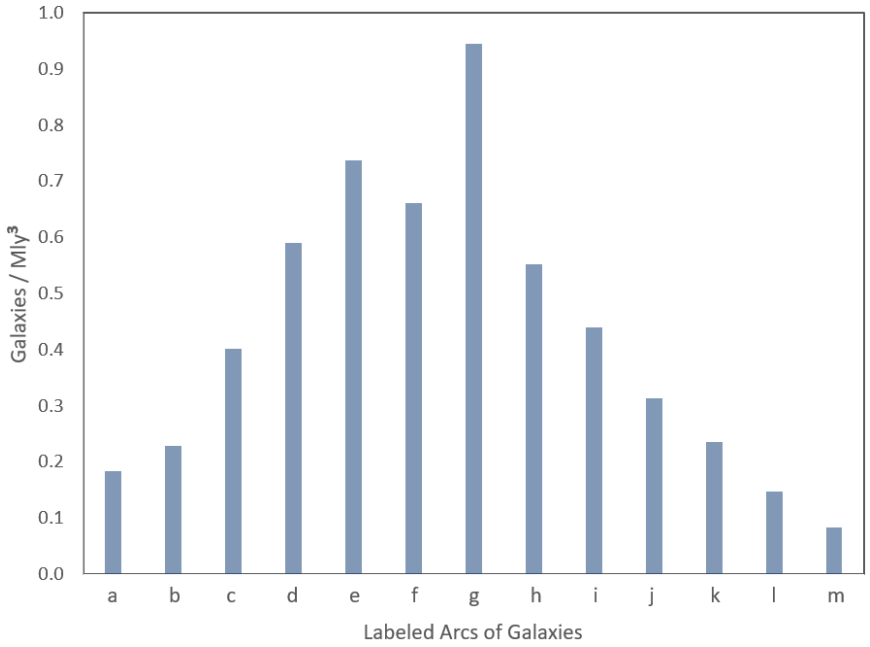

The arc of galaxies labeled *g* has the highest galactic density at 0.95 galaxy/Mly^3 (XI). Galactic density systematically decreases to either side of the *g*-arc. This circular arc of galaxies matches the galactic density pattern for the kernel.

XII. The Kernel in the Superuniverse Space Level

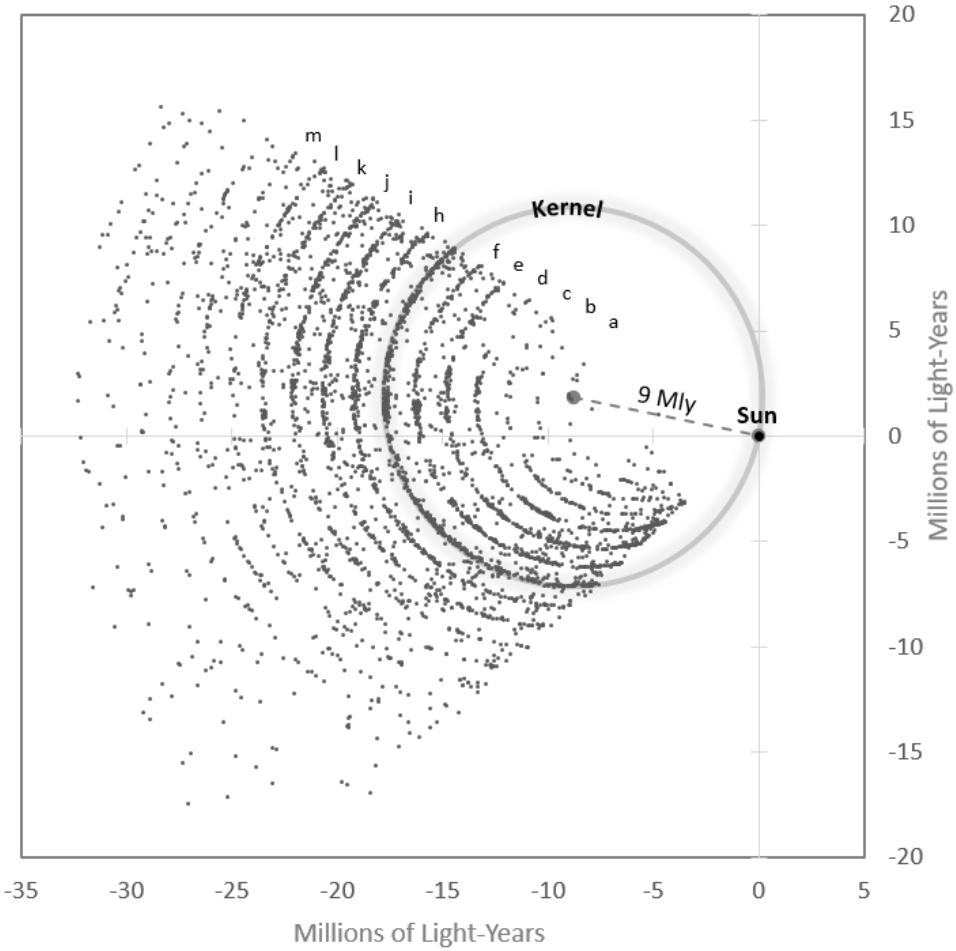

This *g*-arc spans about 150° of a circle, as measured from its center (XII). This circle sweeps around and over Uversa, consistent with the model. The center of this circle is 9 Mly away, which is two percent less than the predicted distance of 9.2 Mly. The *g*-arc has the circular form, galactic density, and size expected for the kernel in the superuniverse space level.

XIII. Identifying the Plane of Creation in the 2dF Belt of Galaxies

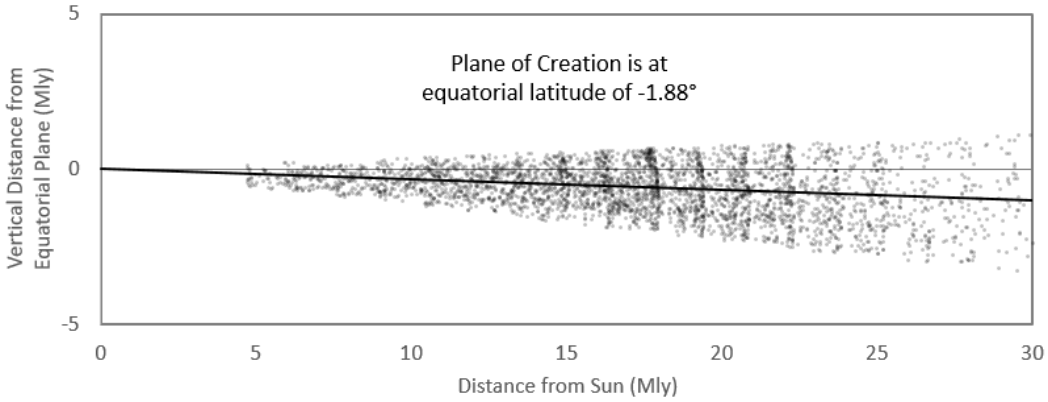

The gravitational revolution of the superuniverse space level requires a balanced distribution of mass above and below the gravitational plane. This plane can be identified by the median latitude of galaxies in the 2dF belt. The median shows the gravitational plane is tilted 1.9° below the equatorial plane.

XIV. Galactic Densities in the 2dF Belt by Horizontal Distance from Paradise Versus Vertical Distance from the Gravitational Plane

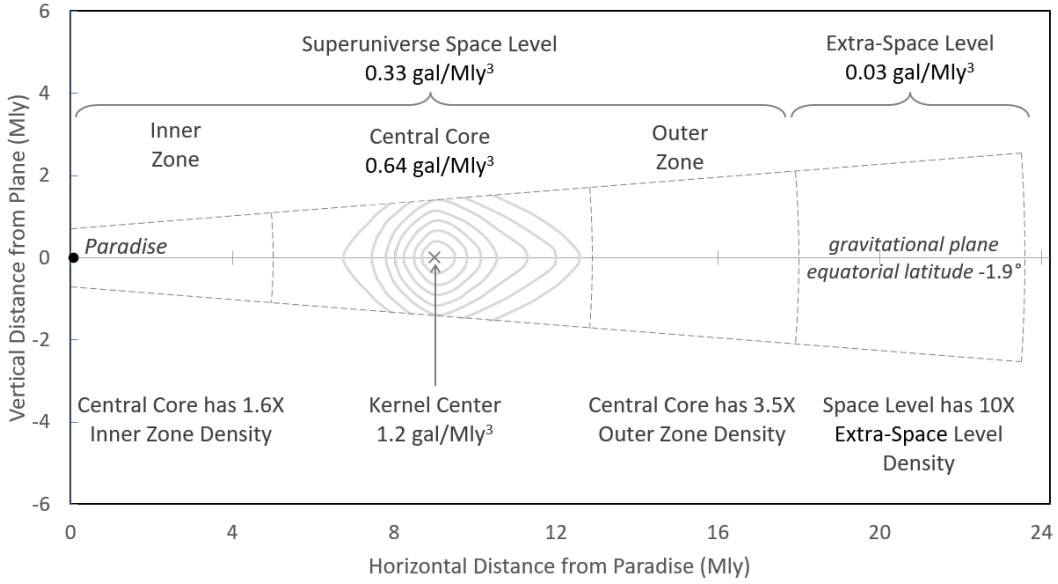

The chart (XIV) plots galactic densities in the 2dF Belt by their horizontal distance from Paradise and their vertical distance above and below this gravitational plane. A maximum density of 1.2 galaxies per cubic million light years occurs in the kernel, which is 9 Mly from Paradise. The kernel is surrounded by concentric regions of progressively decreasing galactic density, matching the two-dimensional density profile for the interior of the central core.

XV. The Central Core in the Superuniverse Space Level

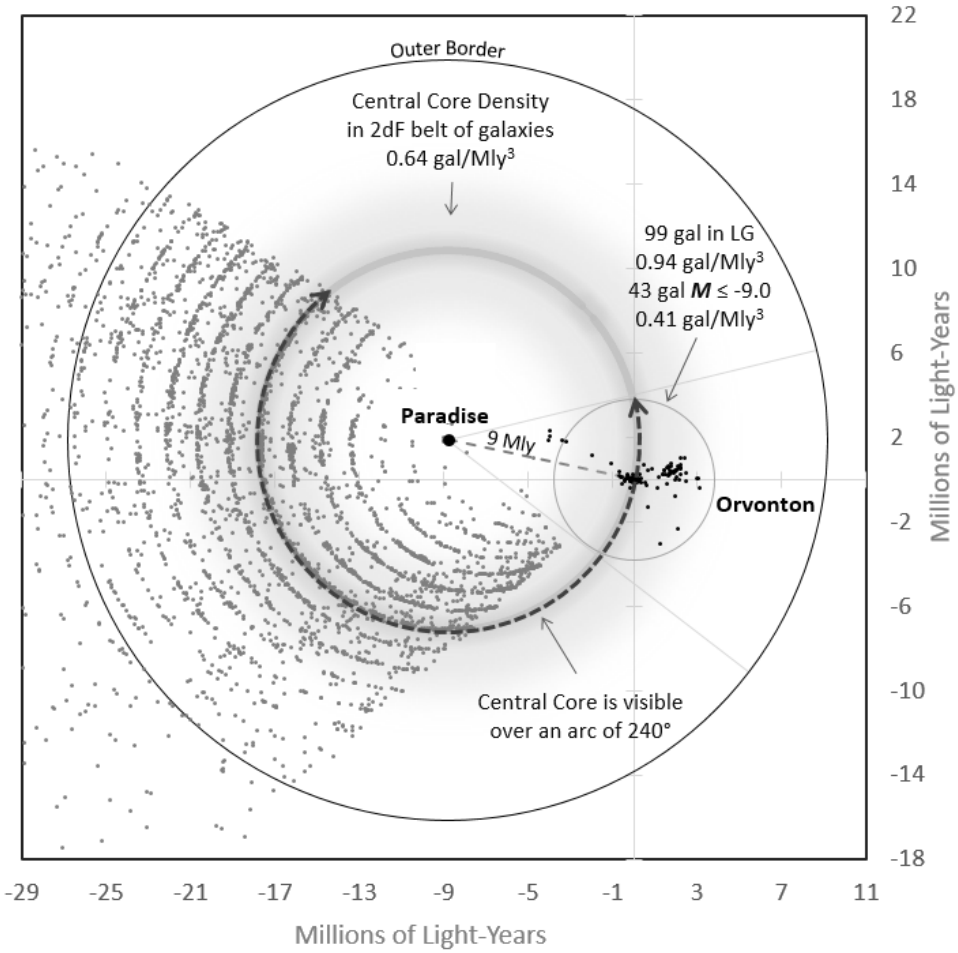

The central core in the 2dF belt (XV) has an average density of 0.64 galaxies per cubic million light-years (XIV). The 99 galaxies in the Local Group have a density of 0.94 galaxies per cubic million light-years (See Appendix). However, only 43 of these galaxies have an inherent brightness (absolute magnitude of $\boldsymbol{M} \leq -9$) strong enough to be seen at the remote distances of the central core (apparent magnitude limit of the 2dF telescope is $\boldsymbol{m} \leq +19.45$). These 43 galaxies have a density of 0.41 galaxies per cubic million light-years, which is comparable to the central core density. This, plus the location of Uversa in the kernel, demonstrates the Local Group is a continuation of the central core. The central core is observable over two-thirds of a circle. It clearly extends over the remaining one-third, almost all of which is hidden behind the belt of stars in the Milky Way.

4. The First Outer Space Level

The first outer space level has the same pattern of organization as the superuniverse space level, except it is 100 times larger. It should have a width of 1.8 billion light-years and its kernel should be 900 Mly from us. Its central core should have a width of 800 Mly. A cosmic structure consistent with these parameters was discovered in 2003.

XVI. The Sloan Great Wall Discovered in 2003

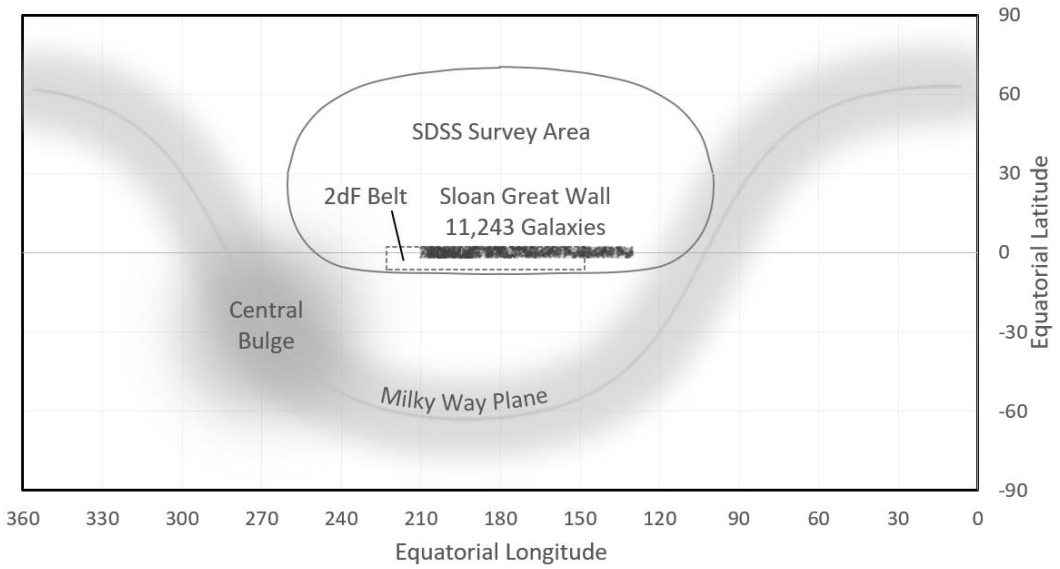

The Sloan Digital Sky Survey [5] has scanned more than one third of the whole sky (XVI). In 2003 J. Richard Gott of Princeton University discovered a belt of galaxies in the SDSS survey data, which he named the Sloan Great Wall. [6] This belt is 80° of longitude in length and extends at least 2° above and below the celestial equator. The outline of this belt of galaxies is clearly observable against the SDSS survey area.

XVII. The 1.4 Billion Light-year long Sloan Great Wall

11,243 Galaxies (Gott 2003)

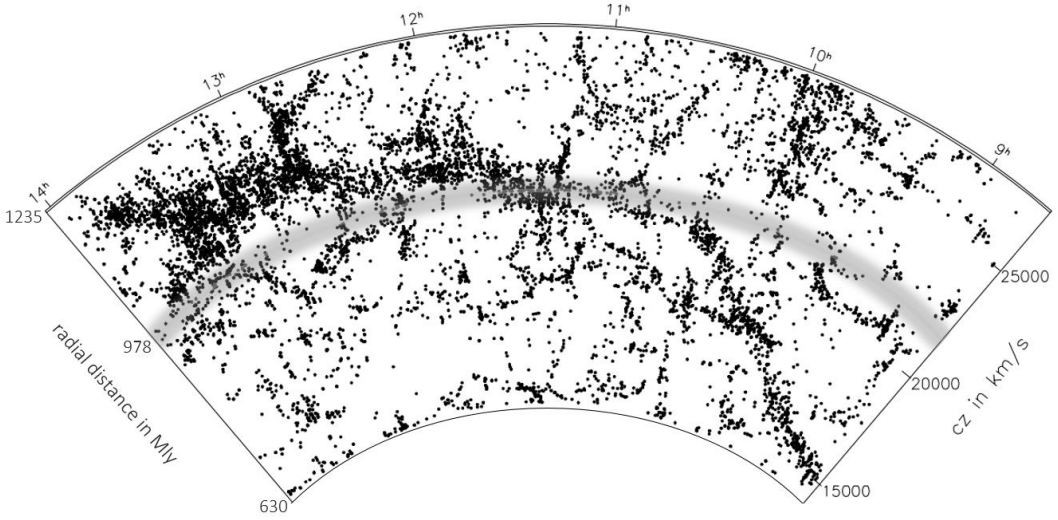

The Sloan Great Wall is a very flat arrangement of galaxies. It is 1.4 billion light-years long and at least 100 Mly high (XVII). It begins at 630 Mly and ends at 1235 Mly. This width of 600 Mly is three-quarters of the expected width of 800 Mly for the central core. Gott finds the median distance for the galaxies in this structure occurs at 978 Mly ($z = 0.073$; Gott assumes $H_0 = 71\ \mathrm{km/s\ Mpc^{-1}}$). This is eight percent farther than the prediction of 900 Mly to the kernel. There are at least seventy thousand aggregations of matter in the central core. [31:10.19] An 80° long section of the central core should contain a minimum of 15,550 galaxies. Gott counts 11,243 galaxies in the Sloan Great Wall, which is three-quarters of this expected number. (Absolute magnitudes of its galaxies: $-19.0 \geq \boldsymbol{M} \geq -22.5$ [7]; only four galaxies in the Local Group are this luminous.)

XVIII. Gravitational Plane of the First Outer Space Level

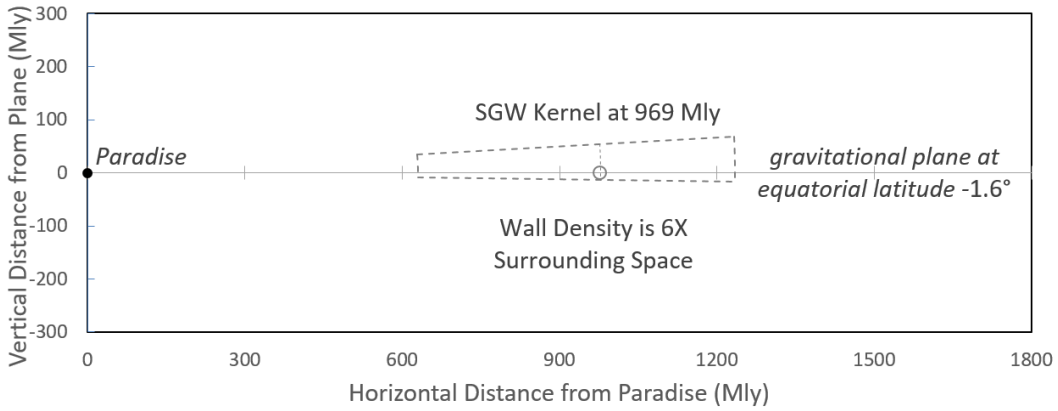

The galactic density in this structure (XVIII) is six times greater than it is in surrounding space. [7] The median latitude of galaxies in the Sloan Great Wall occurs at

−1.63°. The gravitational plane for this structure differs by just 0.25° from the gravitational plane for the 2dF ring of galaxies, which occurs at −1.88°. The Sloan Great Wall and the 2dF ring of galaxies share the same gravitational plane.

PART II: Absolute Gravity and the Redshift-Distance Relation

5. Evidence Suggesting the Hypothesis of a New Type of Gravity

XIX. Sloan Great Wall and 2dF Ring of Galaxies on the Same Plane

(Drawn to Scale)

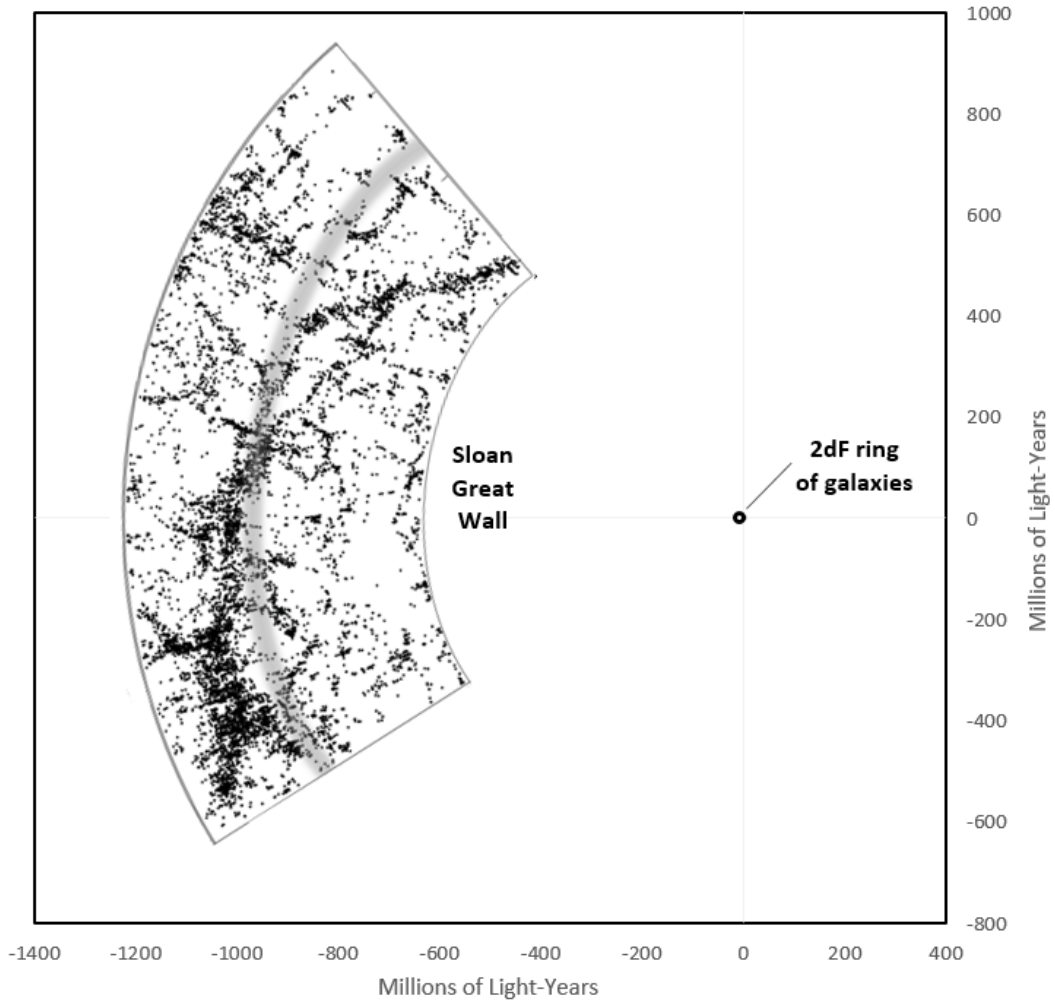

It is highly unlikely the planar organization of galaxies in the Sloan Great Wall is an accident. The same is true for the 2dF ring of galaxies. It is extremely improbable that these two annular structures are also aligned on the same plane by accident (XIX). These

three facts could be explained by gravitational revolution around a common center. For instance, the planar alignment of planetary orbits in our solar system can be explained in this way. But gravity cannot explain the Sloan Great Wall, because there is no observable mass which might act as its gravitational center. The same lack of observable mass is apparent at center of the 2dF ring of galaxies.

The Sloan Great Wall appears to be an accident, because there is no apparent cause for it. Its planar form cannot be explained by the four known or suspected forces capable of moving galaxies. The attractive force of gravity is one. The second is an unnamed repulsive force which initiated space expansion and the universal dispersion of matter (1927). This repelling force cannot move galaxies into the arrangement seen in the Sloan Great Wall. The remaining two are also repulsive forces. The third is the hypothetical force of dark energy, which is required to explain the "accelerating universe" (1998). The fourth is the hypothetical force of inflationary energy, which causes cosmic inflation (1980), a hypothesis required to solve the horizon problem caused by space expansion.

The dynamic of gravitational revolution could explain the Sloan Great Wall, the 2dF ring of galaxies, and their planar alignment, except there is no observable matter at the center of the 2dF ring. On the other hand, it is possible there is a massive body at this location which is composed of a new type of unobservable matter. A very relative precedent for this supposition is the hypothesis of dark matter, which is unobservable.

It was discovered in the 1960s that the orbital velocities of stars in disc galaxies could not be explained. Gravity requires these velocities to steadily decrease as the distance from the center increases. Instead, they remain approximately constant as the distance increases. The presence of dark matter resolves this problem. The hypothesis adds the quantity of mass needed in the way required to enable gravity to explain the flat rotation curves of disc galaxies. Dark matter must be inherently unobservable to fit the facts. It cannot emit, reflect, or absorb electromagnetic energy. It is fundamentally different from atomic or baryonic matter, which interacts with light energy. Dark matter is a non-baryonic type of matter which has mass, like atomic matter, but does not interact with photons.

The standard model assumes the universe is uniformly filled with atomic matter in the beginning. Gravity can explain the formation of stars and galaxies, but it cannot explain the planar form of the Sloan Great Wall. Following well-established precedent, it is supposed there is a new type of unobservable matter at the center of the 2dF ring of galaxies which exerts a new type of central force.

6. Properties of Absolute Gravity

This hypothesis of a new type of gravity is not unusual. Since 1960, over a dozen new theories of gravity have appeared, in response to emerging problems, like the flat rotation curves of galaxies. All are versions of general relativity (except for Modified Newtonian Dynamics), and all model gravity as an inverse-square force. The gravity described in the book is a different type of central force called absolute gravity. It has at least six properties which clearly differentiate it from linear gravity.

XX. Focal Points of Absolute and Linear Gravity

Ellipse major axis of 7 units and minor axis of 6 units

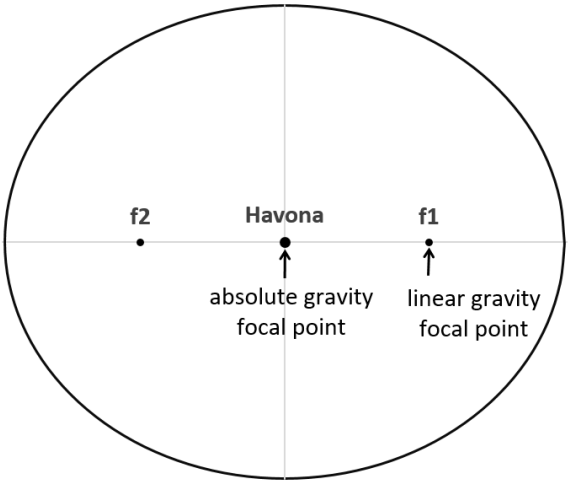

1) *Focal Point of Gravity* (XX): The force of absolute gravity only acts from Paradise, which is its "center and focal point." [11:8.2] Paradise is at the center of Havona, [12:1.10] so the focal point of absolute gravity is the common center for all six elliptical space levels. The focal point of linear gravity in any revolving system is always one of the two focuses of an ellipse.
2) *Mutual Attraction*: Absolute gravity only acts as a central force which attracts the most elementary particles of matter. [42:1.2] It does not cause all particles to be attracted to all other particles in the universe. [41:9.2] The force of linear gravity causes mutual attraction between all particles, as well as acting as a central force in a revolving gravitational system.
3) *Range of Action*: Absolute gravity has a potentially unlimited range of action, because the universe is potentially infinite in extent. [3:4.2] The gravity of Newton and Einstein is repeatedly referred to as "local or linear gravity." Its inverse-square force decreases rapidly with the distance, limiting its range of action.

4) *Force-Mass Relation*: The force of linear gravity is proportional to the mass. The potentially infinite force of absolute gravity is not proportional to mass. Paradise [11:0.1] has a less than infinite mass, since it can be compared to other finite masses. [12:1.10]

XXI. Apsidal Precession under Absolute and Linear Gravity

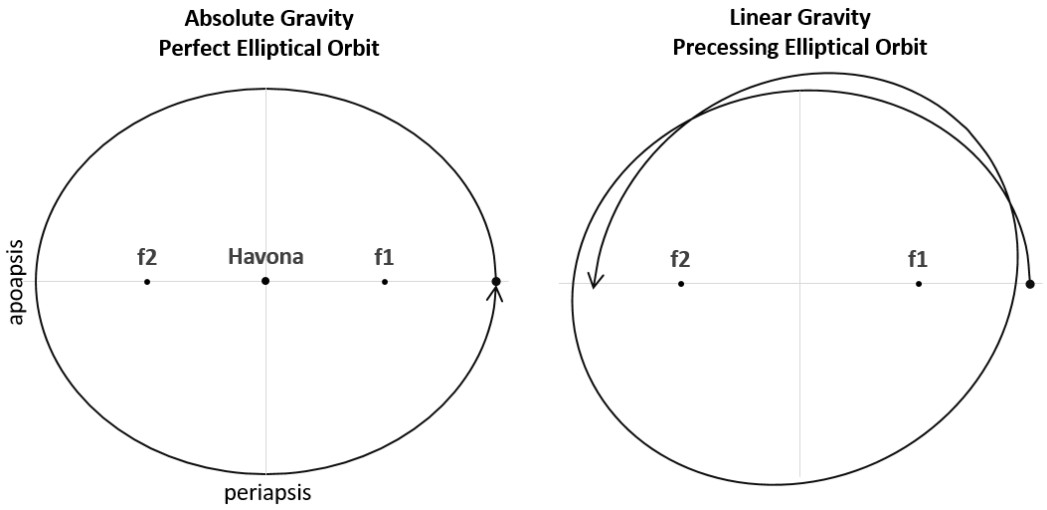

5) *Apsidal Precession* (XXI): Linear gravity produces orbits which exhibit apsidal precession, except in a single satellite system. Apsidal precession is the rotation of the major axis of a satellite's elliptical orbit and is caused by mutual attraction to other satellites in a revolving system. The major axis of the earth's orbit rotates 360 degrees over of a period of 112,000 years. The other planets have different periods of precession. Absolute gravity does not cause apsidal precession. In our orbit around Paradise, we repeatedly return to "the very same space" we "traversed ages ago." [15:1.3] We pursue a perfectly elliptical orbit. Apsidal precession would destroy the concentric arrangement of the six space levels. [12:1.3]

6) *Central Force*: The book compares absolute gravity to the force of elastic tension. "This concept aids us in grasping the fact that everything is drawn inward towards Paradise." [11:8.9] Absolute gravity is like a spring connecting Paradise to each elementary particle. Stretching a spring causes a restoring force that is quantified by the law of elasticity. This restoring force equals a force constant k times the displacement x from a position of equilibrium: $F = -kx$.

XXII. Forms of Simple Harmonic Motion caused by the Force of Elastic Tension

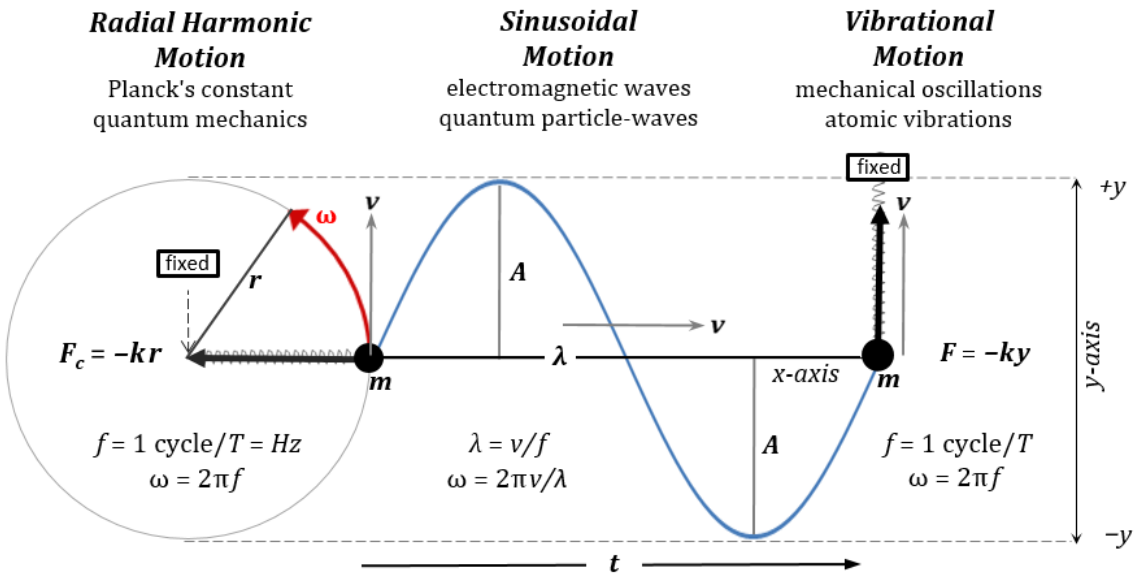

Relevant Equations

$k = \omega^2 m$	$k = \omega / v$	$k = \omega^2 m$
$v = \omega r$	$v = (\omega / 2\pi)\lambda$	$v = \omega A \cos(\omega t)$
$a_c = -\omega^2 r$	$A = v / \omega$	$a = -\omega^2 A \sin(\omega t)$
$KE = \frac{1}{2} m v^2$	$x = A \cos(\omega t)$	$KE = \frac{1}{2} m v^2$
$PE = \frac{1}{2} m \omega^2 r^2$	$y = A \sin(\omega t)$	$PE = \frac{1}{2} m \omega^2 y^2$

The force of elastic tension has a very simple law: Force is directly proportional to distance. It causes a form of periodic motion called simple harmonic motion (XXII). Most notably, the passage of time is scientifically measured by the periodic cycles of simple harmonic motion. Max Planck uses a radial harmonic oscillator to model the quantum of action h which has units of angular momentum L ($h = 6.6\,x\,10^{-34}\,J\,s$, $J\,s = kg\,m^2 s^{-1} = L$). Quantum mechanics relies on Schrodinger's energy equation, in which the potential energy is that of a radial harmonic oscillator ($E = KE + PE \rightarrow E = \frac{p^2}{2m} + \frac{1}{2} m\omega^2 r^2$). Sinusoidal motion models electromagnetic waves and quantum particle-waves. Vibrational motion models a mass on the end of a spring and other types of vibration, including atomic vibrations.

XXIII. Physical Properties of Linear and Absolute Gravity

	Property	*Linear Gravity*	*Absolute Gravity*
1.	Focal Point	focus of ellipse	center of ellipse
2.	Mutual Attraction	yes	no
3.	Range of Action	limited	unlimited
4.	Force vs. Mass	$F \propto$ mass	$F \ not \propto$ mass
5.	Apsidal Precession	yes	no
6.	Central Force	inverse-square	direct-proportion
	Force Law	$F = -\frac{GMm}{r^2}$	$F = -kr$
	Potential Energy	$PE = -\frac{GMm}{r}$	$PE = \frac{1}{2}kr^2 = \frac{1}{2}m\omega^2 r^2$
	Gravitational Potential	$V = \frac{PE}{m} = -\frac{GM}{r}$	$V = \frac{PE}{m} = \frac{1}{2}\omega^2 r^2$

The sixth property of absolute gravity describes a directly proportional central force. Absolute gravity causes universal revolution, so this type of central force must support stable periodic orbits. In his *Principia* (1687) Newton provides a geometric proof that an inverse-square central force acting from the focus of an ellipse can sustain periodic orbits (XXIII). [8] He gives a second geometric proof that a directly proportional central force acting from the center of an ellipse also supports periodic orbits. [9] These are the only two he identifies as capable of doing this. Two centuries later, the French mathematician Joseph Bertrand considered all possible types of central force which can support the periodic orbit of a satellite. Bertrand's theorem is an analytic proof demonstrating that these two central forces are the only ones capable of doing this. [10] By these geometric and analytic proofs, absolute gravity can only be a directly proportional central force.

A directly proportional central force is consistent with the first property of absolute gravity, since it acts from the center of an ellipse. This force increases with distance and has a theoretically unlimited range of action, consistent with the third property. It arises from a tension *between* two masses and does not depend on the masses involved, consistent with the fourth property. Newton analyzed the orbits produced by an inverse-square force in a system with multiple satellites. [11] He found that all orbits undergo apsidal precession at different rates, destroying perfectly elliptical orbits. Under a direct-proportion central force, he found that all orbits are perfectly elliptical, consistent with

the fifth property. In Newton's many-body analysis, he assumes a direct-proportion force causes mutual attraction between all bodies in a system. He found this increases the orbital velocities of satellites but does not change their perfectly elliptical orbits. Without the assumption of mutual attraction, satellites orbits and velocities are identical to those calculated in a single satellite system. This is consistent with the second property of absolute gravity, which requires it to act exclusively as a central force.

7. Explaining the Redshift-Distance Relation

These six properties conclusively identify absolute gravity as a directly proportional central force. This central force can explain universal revolution. But in the standard model, galaxies are receding from us at ever-increasing velocities due to the universal expansion of space. Galaxies cannot be in stable periodic orbits around a fixed location in the universe, if they are continuously accelerating away from us.

XXIV. Wavelength Increases in Proportion with Recessional Velocity

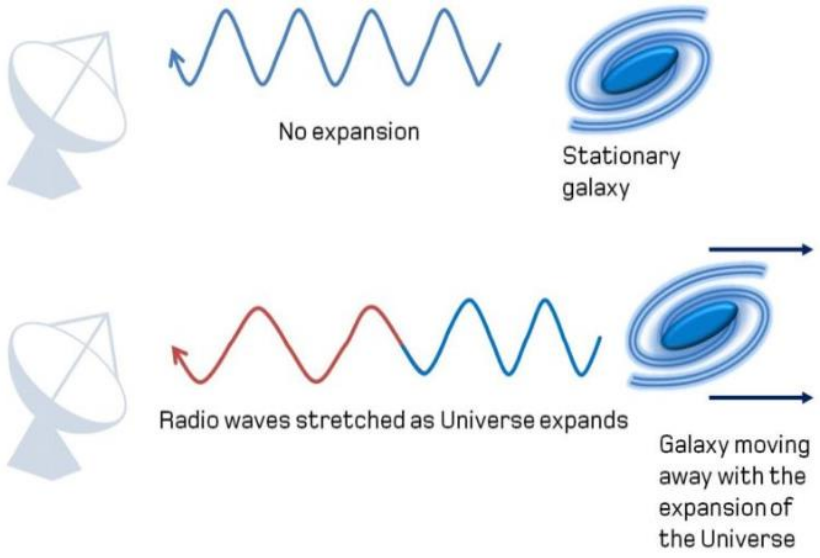

Credit: Square Kilometer Array Project

The concept of an expanding universe is based on the evidence provided by the redshift-distance relation, discovered by Edwin Hubble in 1929. The more distant a galaxy is, the more its light is shifted toward longer wavelengths, redshifted. The redshift-distance relation is the simple observation that galactic redshifts increase in direct proportion to their distances. Hubble suggested this can be explained by a Doppler shift, since this mechanism causes wavelength to increase in direct proportion to receding velocity (XXIV). Velocities increasing directly with distance explain the redshift-distance

relation. This velocity-distance explanation for cosmological redshift is the basis for the expansionary model.

The velocity-distance relation results in many galactic redshifts equating to superluminal velocities. Not all astronomers are convinced such velocities are real. By 1947 Hubble had changed his mind. He thought his velocity explanation for galactic redshifts is probably incorrect, based upon his further observations. [25] His objections prompted others to design critical tests to empirically determine if the universe is expanding or not. Numerous implementations of these critical tests have yielded inconclusive results. [21] Whether the universe expands or not remains undetermined.

The book discusses the relation between redshift and velocity. It says using cosmological redshift to calculate velocity can result in unbelievable speeds in excess of 30,000 miles per second (48,000 km/s). It flatly states "this apparent speed of recession is not real." 12:4.14 Galaxies are not receding from us at these calculated velocities. Galactic redshifts are the result of numerous factors, including "time-space distortions." The greatest distortion is said to arise from the revolution of the space levels. 12:4.15 Since this revolution is caused by absolute gravity, it is clearly implied that galactic redshifts are primarily the result of time-space distortions caused by absolute gravity. These distortions can only refer to relativistic physics, since time and space are ideal realities in classical physics. Relativity theory led to the discovery that gravity causes changes in time, which results in redshifts. It is reasonable to suppose that absolute gravity also causes changes in the passage of time.

8. The Postulates of Special Relativity and Time Dilation

The discovery that gravity causes redshift emerges from Einstein's theory of special relativity. This theory describes how velocity alters the relationships between time, space, energy, and matter. It has two postulates. The first postulate states the laws of physics are the same in all inertial frames. Einstein incorporates Newton's concept of relative inertial frames, but excludes his postulates of absolute space and absolute time. Newton's inertial frame begins as an ideal abstraction of Euclidean geometry. Newton gives this abstraction materiality by appealing to Aristotle's metaphysical notion of natural places and motions. The natural place of the universe is the whole of space and the natural motion of absolute space is to be at rest. A relative inertial frame is a moving place or part of absolute space. It is, therefore, natural for this moving place to oppose any actions which might change its resting motion in absolute space. Inertia (*vis inertiae*) is the natural motion of absolute space, and it endows inertial frames with concrete reality. Inertia

characterizes material bodies, because they are places which occupy volumes of absolute space. Absolute time and the absolute inertial resistance of matter to action are the metaphysical foundations of Newton's physics and his three laws of motion.

Einstein discards absolute space and replaces absolute time with an absolute constant of motion. The second postulate states the speed of light through empty space is absolutely constant in all inertial frames. In his physics, the motion of light defines time, instead of time defining the motion of light. ("Time comes by virtue of motion." [12:5.1]) The speed of light is the same in every inertial frame, and so time is the same in each, in agreement with classical physics. But the rate at which time passes in a moving inertial frame is different from its rate in a stationary frame. When measured from a stationary frame, light emitted from within a moving frame has exactly the same speed as light emitted within the stationary frame. In Newton's physics, the measured speed of light emitted in a moving frame must be different, because it is sum of the speed of the moving frame and the speed of light. In classical physics the speed of light varies, because time is a universal constant. In relativistic physics time varies, because the speed of light is a universal constant. Physics describes the motion of matter in time, and the relativity of time requires a corresponding relativity of distance, mass, and energy. The book validates this astonishing insight of special relativity to the extent of directly confirming its most famous equation, $E = mc^2$. [42:4.11]

XXV. Uniform Velocity Results in Time Dilation

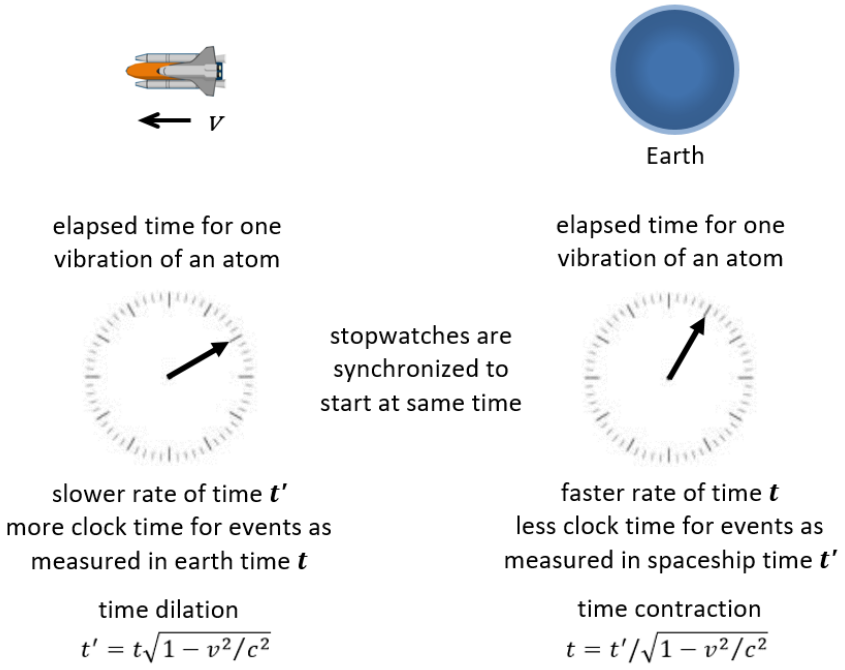

In relativistic physics predictable processes have the same duration in all inertial frames. Atomic clocks measure a second of time by a specific number of cesium atom vibrations. The number of atomic vibrations per second is exactly the same within all inertial frames. However, if one inertial frame is moving relative to a second frame, the rate of time in the moving frame slows down, dilates, when it is measured from the stationary frame (XXV). Time dilation causes the number of vibrations in a moving clock to be less over a second of time measured by a stationary clock. A stationary observer measuring the duration of a predictable event in a moving inertial frame sees it takes more time for it to occur in the moving frame. The faster a clock moves, the more stationary time it takes for physical events to occur in the frame of the moving clock.

XXVI. Equivalence of Uniform and Gravitational Acceleration

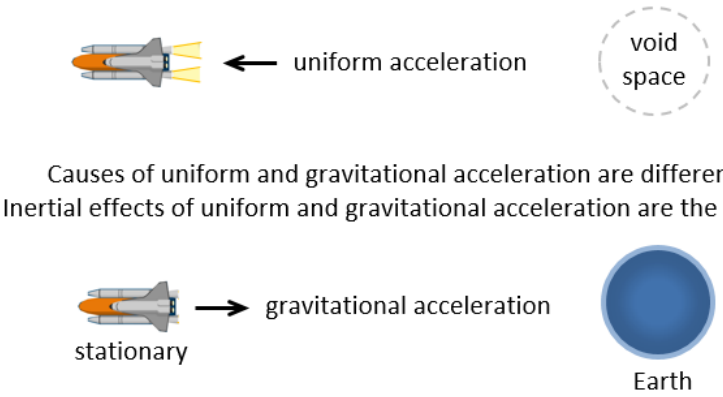

The first postulate of special relativity includes acceleration, the rate of change in velocity. A couple of years after the theory was published, Einstein realized that uniform acceleration is equivalent to gravitational acceleration (XXVI). (Einstein gives a personal account of how he arrived at the theory of relativity and the equivalence principle in a 1922 speech. [12]) The inertial effects in a uniformly accelerating spaceship are identical to the inertial effects in a stationary spaceship that is being accelerated by gravity. This equivalence led to Einstein to consider the relativistic effects caused by a constant uniform acceleration.

9. Gravitational Redshifts Caused by Linear Gravity

XXVII. Time Dilation Caused by Uniform Acceleration

$$\frac{t}{\boldsymbol{\tau}} = 1 + \frac{ad}{c^2} \qquad (1)$$

t local clock rate at a distance d from the center

$\boldsymbol{\tau}$ system clock rate at center of accelerated frame

a uniform acceleration

d distance between the two clocks

c^2 speed of light squared

Uniformly Accelerated Inertial Frame

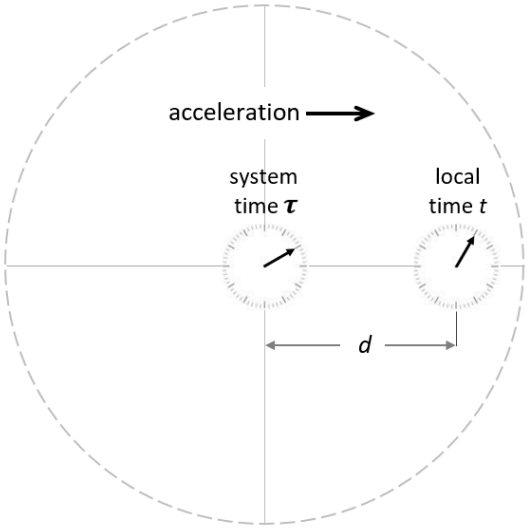

Einstein analyzes the effect of uniform acceleration on the passage of time in a 1907 monograph on special relativity. [13] He considers an experimental setup with one clock at the center of an inertial frame and a second clock some distance from this center (XXVII). He assumes this inertial frame has a uniform acceleration and synchronizes the two clocks using the equations of special relativity. Solving these equations gives the ratio of the two clock rates; that is, how much faster one clock runs than the other. This time dilation equation shows that the local rate of time t at a distance d from the center is faster than the system rate of time $\boldsymbol{\tau}$ at the center (1). Conversely, system time is slower than local time.

XXVIII. Time Dilation and Redshift Caused by Linear Gravity

$$\frac{t}{\boldsymbol{\tau}} = 1 + \frac{ad}{c^2} \qquad \textit{Uniform acceleration time dilation} \qquad (1)$$

$$\frac{t}{\boldsymbol{\tau}} = 1 + \frac{V}{c^2} \qquad \textit{Time dilation as a function of field potential} \quad \text{since } V = ad \qquad (2)$$

$$\frac{t}{\boldsymbol{\tau}} - 1 = \frac{a_c r}{c^2} \qquad \textit{Time dilation as a function of central force potential} \quad \text{since } a_c = a \text{ and } r = d, \text{so } V = a_c r \qquad (3)$$

$$\frac{t}{\boldsymbol{\tau}} - 1 = \frac{GM}{rc^2} \qquad \textit{Time dilation as a function of linear gravitational potential} \quad \text{since } \frac{GM}{r} = \Phi \text{ equivalent to } a_c r = V \qquad (4)$$

$$z = \frac{GM}{rc^2} = \frac{\Phi}{c^2} \qquad \textit{Linear gravity redshift equation} \quad \text{since } z = \frac{\lambda_o}{\lambda_e} - 1 = \frac{f_e}{f_o} - 1 = \frac{t}{\boldsymbol{\tau}} - 1 \qquad (5)$$

The equivalence of uniform and gravitational acceleration extends to their field potentials. Uniform acceleration times some distance creates a vector field potential V relative to the center of the accelerated frame (2) (XXVIII). (Vector fields describe the potential energy intensity of phenomena like electric, magnetic, and gravitational forces.) In Einstein's thought experiment, uniform acceleration is constant, so the field potential it creates increases from zero at the center of the frame, since a zero radius has a zero potential (3): $V = a_c r$. The field potential Φ created by linear gravity increases from a maximum negative intensity at the center of the field to zero at an infinite distance (4): $\Phi = -GM/r$. The two field potentials are equivalent, since both increase positively from a minimum to a maximum as the distance from the center increases. The gravitational potential of linear gravity equals the gravitational constant G times a central mass M divided by the radius r. Einstein makes this substitution to get the first order time dilation equation for linear gravity (4).

Acceleration causes time dilation which results in redshift. The ratio of local time divided by system time at the center is equivalent to the ratio of the frequency f_e of light emitted at some distance from the center divided by the frequency f_o observed at the center. This is identical to the ratio of the wavelength λ_o observed at the center divided by the wavelength λ_e emitted at this distance. Making this substitution, Einstein arrives at the gravitational redshift equation (5). It is notable that this equation can be derived exclusively from special relativity without relying on the equivalence principle or the curved spacetime geometry of general relativity. [14]

XXIX. Gravitational Redshift and Time Dilation

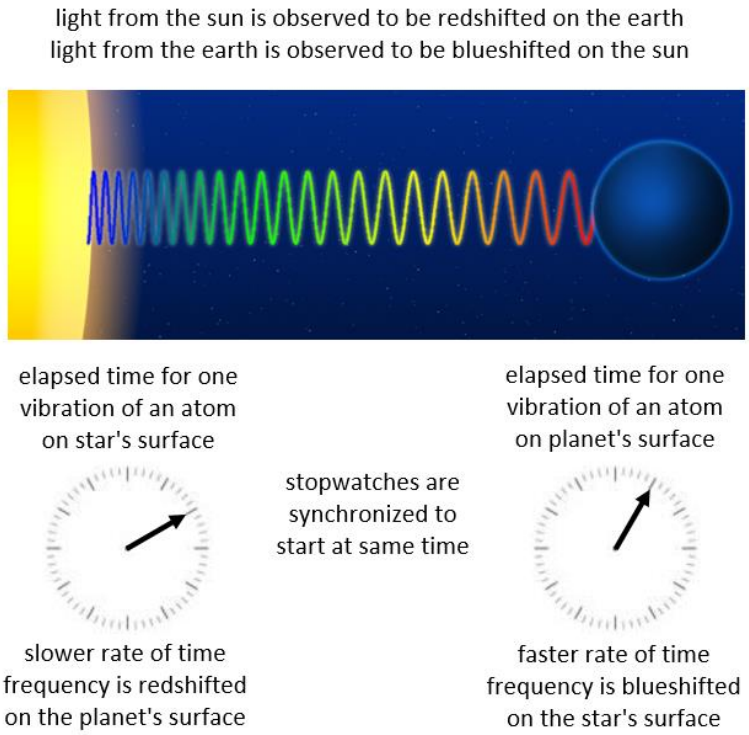

The equivalence principle allows Einstein to translate the time dilation caused by uniform acceleration to gravitational acceleration. The identity of time dilation and redshift yields the gravitational redshift equation. Einstein uses this equation (5) to successfully predict that light emitted from the surface of the sun is redshifted by two parts in a million (XXIX). His gravitational time dilation equation (4) is used in the Global Positioning System to make ongoing time corrections to the atomic clocks in the system. [15] GPS satellites are about 12,000 miles above the earth. The weaker gravitational acceleration at this height causes cesium atoms in atomic clocks to vibrate faster than they do at sea level. A 24 hour period on these satellites is 45.6 microseconds less than 24 hours measured by a clock on the earth's surface. Time runs a little faster on these satellites.

10. Gravitational Redshifts Caused by Absolute Gravity

XXX. Acceleration, Distance and Redshift Proportionalities

$$z \propto r \qquad \textit{Uniform acceleration redshift-distance relation} \quad \text{since } z = \frac{a_c}{c^2}\, r \text{ and } a_c \text{ and } c^2 \text{ are constant} \tag{6}$$

$$z \propto \frac{1}{r} \qquad \textit{Linear gravity redshift equation} \quad \text{since } z = \frac{GM}{rc^2} \text{ and } \frac{GM}{c^2} \text{ is constant} \tag{7}$$

$$\sqrt{a_c} \propto \frac{1}{r} \qquad \textit{Linear gravity acceleration equation} \quad \text{since } a_c = \frac{GM}{r^2} \tag{8}$$

$$z \propto \sqrt{a_c} \qquad \textit{Linear acceleration-redshift relation} \quad \text{since } z \propto \frac{1}{r} \text{ and } \sqrt{a_c} \propto \frac{1}{r} \tag{9}$$

Special relativity shows that acceleration causes time dilation and redshift. The redshift equation for uniform acceleration (6) holds in the general case, because it does not depend on the cause of acceleration (XXX). In Einstein's thought experiment uniform acceleration is constant, and redshift is directly proportional to the radius $z \propto r$ (6). This changes in the redshift equation for linear gravity (7), where redshift is inversely proportional to the radius $z \propto 1/r$. This change occurs, because the acceleration of linear gravity varies inversely with the square of the distance (8). This force law causes the square root of the acceleration to be inversely proportional to the radius. Since acceleration and redshift have the same relationship with the radius, redshift is directly proportional to the square root of the acceleration (9).

XXXI. Acceleration-Radius Proportion for Absolute Gravity

$$F = -kr \qquad \textit{Law of absolute gravity} \qquad (10)$$

$$a_c = -\frac{k}{m}r \qquad \text{since} \quad a = \frac{F}{m}$$

$$a_c = -\omega^2 r \qquad \textit{Absolute acceleration equation} \quad \text{since} \quad \omega^2 = \frac{k}{m} = \text{constant} \qquad (11)$$

$$a_c \propto r \qquad \textit{Acceleration-radius proportion} \qquad (12)$$

Absolute gravity has a different force law (10). This law causes acceleration and redshift to have a common relationship with the radius that is different from linear gravity. The force of absolute gravity equals a force constant k times the radius (XXXI). (k has units of kg/s^2.) Acceleration is found by dividing both sides of this force equation by unit mass. In radial harmonic motion the force constant k divided by unit mass equals the square of the angular velocity ω. (Angular velocity has units of radians per second θ/s.) Making this substitution, the centripetal acceleration equals the angular velocity squared times the radius (11). Since angular velocity squared ω^2 is a constant in radial harmonic motion, the acceleration is directly proportional to the radius (12).

XXXII. Proportionalities for Linear and Absolute Gravity

Linear Gravity	*Absolute Gravity*	
$\sqrt{a_c} \propto \frac{1}{r}$	$a_c \propto r$ since $a_c = -\omega^2 r$	(12)
$z \propto \frac{1}{r}$	$z \propto r$ since $a_c \propto r$	(13)
$z \propto \sqrt{a_c}$	*Absolute acceleration-redshift relation* $z^2 \propto a_c$ $z^2 = \frac{a_c r}{c^2}$ since $a_c r = (\omega^2 r) r$ and $z \propto r$	(14)

The acceleration is directly proportional to the radius under absolute gravity (12) (XXXII). Its central force law requires redshift and acceleration to have the same relation to the radius, so redshift must also be proportional to the radius $z \propto r$ (13). This is the same as the redshift-distance relation that is found for a constant uniform acceleration (6). But acceleration varies with distance in absolute gravity $a_c = \omega^2 r$, instead of being constant. Substituting this varying acceleration in the field potential equation for uniform acceleration $V = ad$ (4) causes redshift to be proportional to the square of the radius $z =$

$(\omega^2 r)r$. The force law of absolute gravity requires redshift and acceleration have the same proportionality to distance, and redshift must be squared to match the square of the radius (14). The acceleration-redshift relation for absolute gravity is the square of the acceleration-redshift relation for linear gravity (9).

XXXIII. Redshift Equation for Absolute Gravity

$$z = \frac{V}{c^2} \qquad \textit{Redshift equation for uniform acceleration} \qquad (5)$$

$$\Phi = \frac{1}{2} a_c r \qquad \textit{Radial harmonic gravitational potential} \text{ since } \Phi = V \qquad (15)$$

$$z^2 = \frac{1}{2}\frac{a_c r}{c^2} \qquad \text{since } z^2 = \frac{a_c r}{c^2} \ (14) \qquad (16)$$

$$z^2 = \frac{1}{2}\frac{\omega^2 r^2}{c^2} \qquad \textit{Absolute gravitational redshift equation} \text{ since } (\omega^2 r)r = a_c r \qquad (17)$$

The redshift for uniform acceleration equals its field potential divided by the square of the speed of light (5) (XXXIII). The gravitational field potential for absolute gravity is defined by radial harmonic motion and equals one-half the centripetal acceleration times the radius (15). Making this substitution, redshift equals this gravitational potential divided by the speed of light squared (16). Redshift is squared in this equation so that it is directly proportional to the radius. The acceleration equals the angular velocity squared ω^2 times the radius (11). Making this substitution gives the redshift equation (17) a form parallel to that for the linear gravity (5). The angular velocity squared ω^2 is a constant in this equation and plays the same role as the gravitational constant does in the linear gravity equation.

The acceleration of absolute gravity increases in direct proportion to the radial distance. This linear increase in centripetal acceleration with distance causes a linear increase in redshift with distance. Under the hypothesis of absolute gravity, cosmological redshift must be a gravitational redshift, because special relativity proves acceleration causes time dilation and redshift in the general case.

11. A Critical Test of the Hypothesis of Absolute Gravity

XXXIV. The Absolute Velocity of the Milky Way

Polar view of Superuniverse Space Level

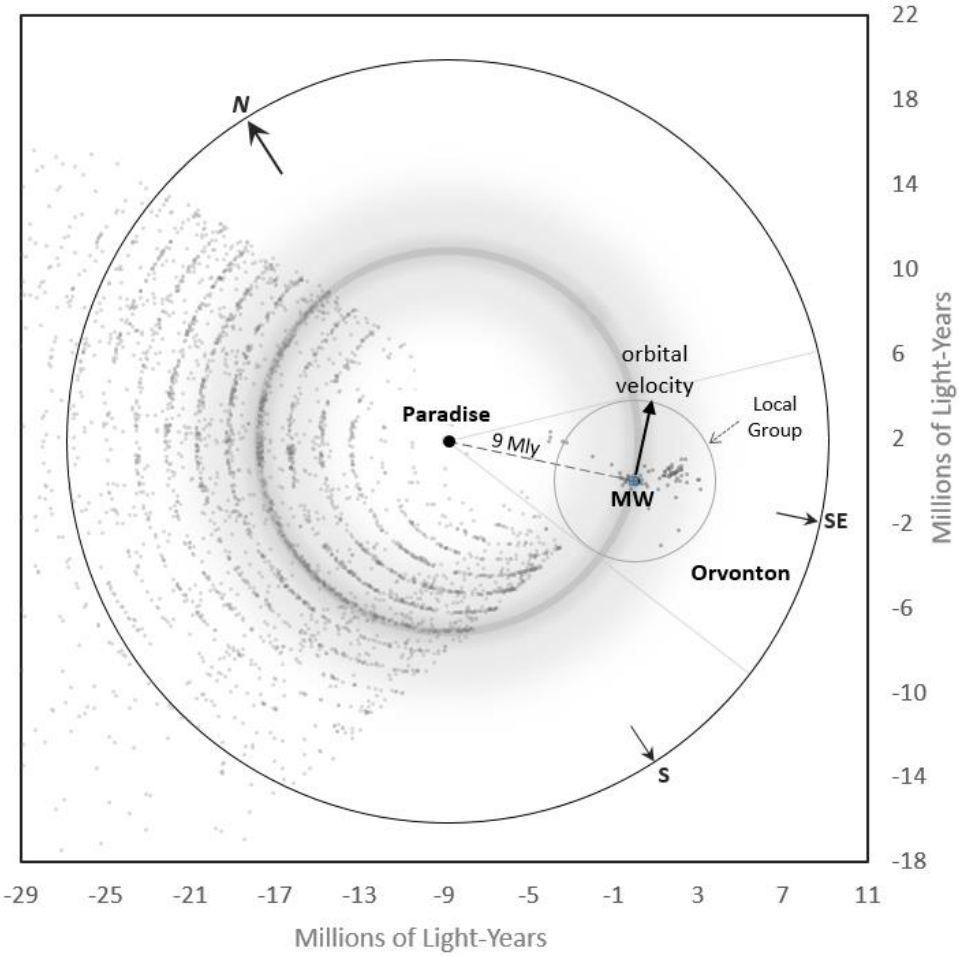

The annular forms and planar alignment of the 2dF ring of galaxies and the Sloan Great Wall are circumstantial evidence of absolute gravity and an unobservable cosmic body at the center of the 2dF ring. This structural evidence for the location for the Isle of Paradise would be significantly strengthened by dynamic evidence of revolution around this location. If absolute gravity explains these structures, its force law can predict the orbital velocities of galaxies around this center.

In the new model, the Milky Way "represents the central nucleus of Orvonton." [15:3.1] It is located at the center of the Local Group (XXXIV), since it is right next to Uversa. The Milky Way is 9 Mly ($D = 2.76$ Mpc) from Paradise, which equals $8.5\ x\ 10^{19}$ kilometers ($9.46\ x\ 10^{12}$ km/ly). The rate of space expansion (Hubble constant H_0) within 23 Mly has been measured at 67 km/s per megaparsec, [17] when expressed in terms of the velocity-

distance relation. At this rate and distance, the standard model calculates a velocity of recession equal to 185 km/s ($v = H_0 D = 67 \frac{\text{km}}{\text{s}}/\text{Mpc} \cdot 2.76\,\text{Mpc}$). This receding velocity corresponds to a cosmological redshift of $z = 0.000617$ ($z = v/c = 185\ \frac{km}{s}/299792\,\frac{\text{km}}{\text{s}}$).

XXXV. Predicted Orbital Velocity of the Milky Way

Polar view of Superuniverse Space Level

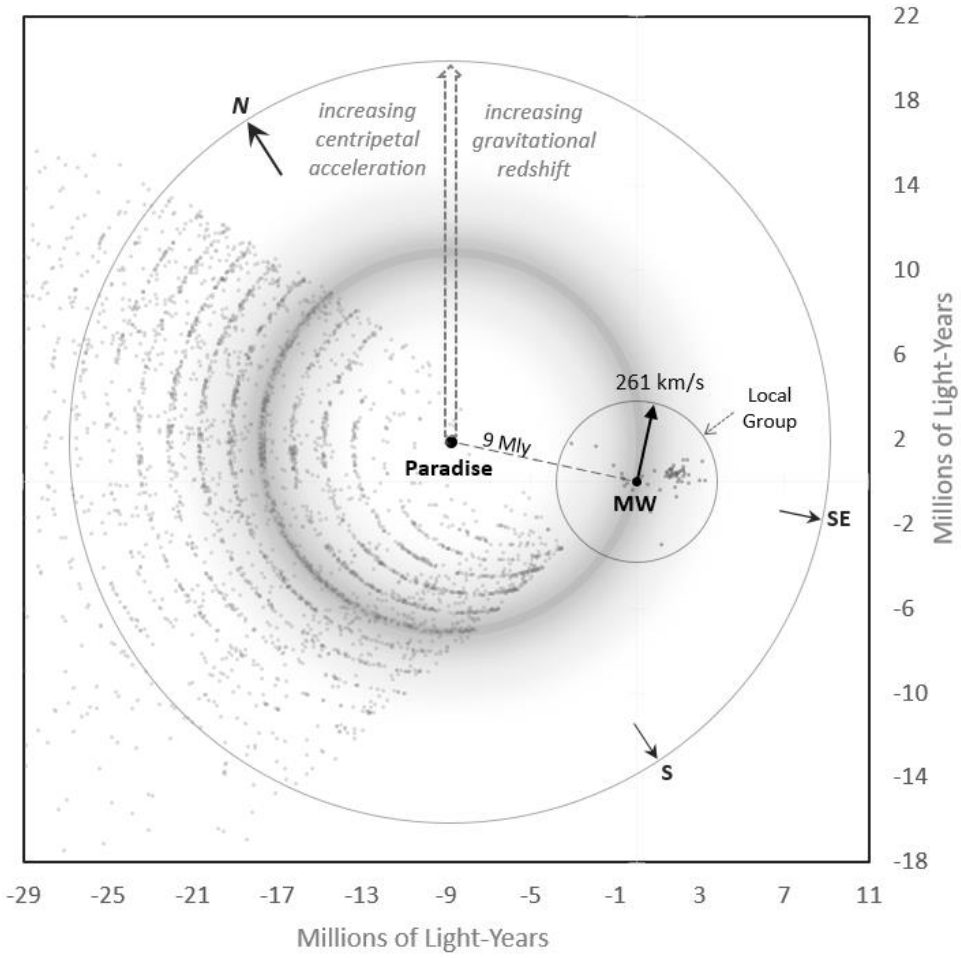

In the hypothesis of absolute gravity, cosmological redshift is not caused by receding velocity. It is caused by a gravitational potential emanating from Paradise, where this potential is zero ($\Phi = \frac{1}{2}\omega^2 r^2,\ \Phi \to 0 \text{ as } r \to 0$). The Milky Way is 9 Mly from the center of this gravitational potential. The gravitational potential at this distance from Paradise gives the Milky Way a cosmological redshift that is equivalent to 185 km/s in the standard model. In the standard model, the Milky Way cannot have a cosmological redshift, because the Milky Way is at the center of expansion. Space expansion occurs from every location in the universe; there is no preferred center.

XXXVI. Predicted Orbital Velocity of the Milky Way

$$z^2 = \frac{1}{2}\frac{a_c r}{c^2} \qquad \textit{Absolute gravitational redshift} \tag{17}$$

$$a_c = \frac{2c^2 z^2}{r} \qquad \textit{Absolute acceleration}$$

$$a_c = \frac{2\left(299792\,\frac{\text{km}}{\text{s}}\right)^2 (0.000617)^2}{8.51\ x\ 10^{19}\ \text{km}} = 8.03\ x\ 10^{-16}\ \frac{\text{km}}{\text{s}^2} \tag{18}$$

$$\omega^2 = \frac{a_c}{r} \qquad \textit{Absolute angular velocity}$$

$$\omega^2 = \frac{8.03\ x\ 10^{-16}\ \frac{\text{km}}{\text{s}^2}}{8.51\ x\ 10^{19}\ \text{km}} = 9.43\ x\ 10^{-36}\ \frac{\theta^2}{\text{s}^2} \tag{19}$$

$$v_o = \sqrt{\omega^2 r^2} \qquad \textit{Absolute orbital velocity}$$

$$v_o = \sqrt{9.43\ x\ 10^{-36}\frac{\theta^2}{\text{s}^2} \cdot 7.25\ x\ 10^{39}\ \text{km}^2} = 261\ \frac{\text{km}}{\text{s}} \tag{20}$$

The absolute gravitational redshift of the Milky Way and its distance from Paradise are known. These are two of the three variables in the gravitational redshift equation (17), which can be rearranged (XXXVI) to solve for the acceleration (18). The angular velocity is then calculated from the acceleration and distance (19). In radial harmonic motion the orbital velocity v_o equals the square root of the angular velocity squared times the radius squared (20). A galaxy 9 Mly from Paradise has an orbital velocity of 261 km/s. This predicted velocity for the Milky Way is parallel to the gravitational plane defined by the 2dF ring of galaxies and perpendicular in a counterclockwise direction to a line drawn to the center of this ring.

(Compass directions proceed clockwise from north (0°) to east (90°). Uversa has moved in a counterclockwise direction from Paradise south (180°) to southeast (135°). [15:1.5] Chart XXXV is assumed to be a polar view of the superuniverse space level, based on the direction of the CMB dipole, which passes "just underneath nether Paradise" at a depth of 790,000 light-years. [11:6.2])

This prediction is a critical test of the hypothesis of absolute gravity. It requires that a centripetal acceleration toward Paradise causes this velocity and also causes a cosmological redshift relative to Paradise. The Milky Way will only have this predicted velocity, if these assumptions are correct. If this prediction is wrong, these assumptions are incorrect.

XXXVII. Absolute Revolution of the Superuniverse Space Level

One revolution every 64.8 billion years

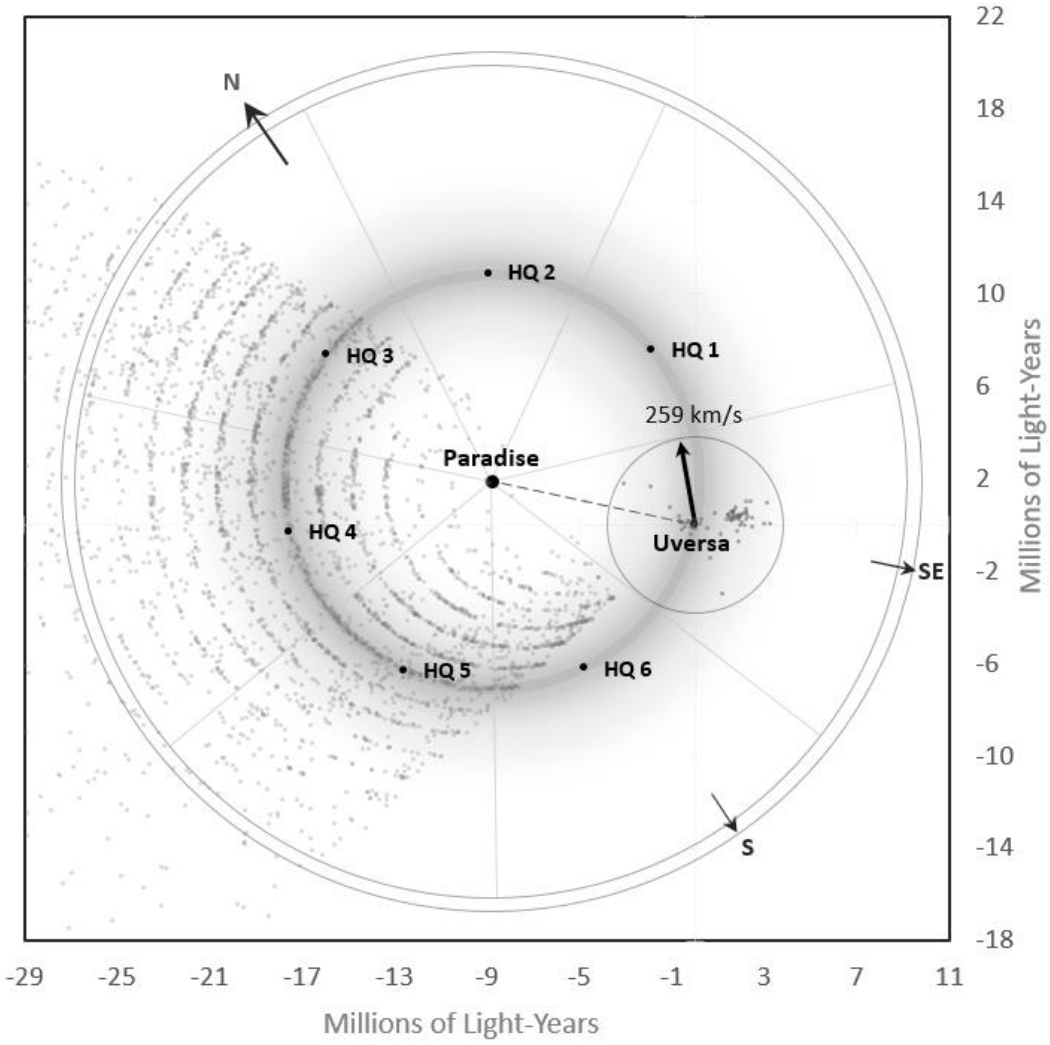

This prediction was untestable until just recently. In 2007 astronomers determined the velocity of the Milky Way in a region referred to as the Local Velocity Field, which extends out to 130 Mly (40 Mpc). This major study examined the bulk motions of galactic clusters within this region which are not caused by universal space expansion. [16] The study identified an expanding collection of galaxies called the Local Sheet, which extends out to 23 Mly (7 Mpc). The Local Group is at the center of this new structure, and the study counts 158 galaxies in it, not including the galaxies in the Local Group. [18] The Milky Way is located at the center of this massive expanding structure. [19] The study found that the bulk motion of the center of the Local Sheet, where the Milky Way is located, is 259 $\pm$ 25 km/s (XXXVII).

This velocity is named the Local Velocity Anomaly, because it has no apparent cause. Other bulk motions in the Local Velocity Field can be explained by the gravitational attraction of large aggregations of galaxies. There is no collection of galaxies large enough to cause this anomalous velocity. In the absence of any other explanation, the study supposes a large empty region called the Local Void is pushing the Local Sheet away at this velocity. This explanation relies on a hypothesis that space expansion is faster in void regions than it is universally. A faster rate of space expansion in the Local Void (90 vs. 74 $\mathrm{km/s\ Mpc^{-1}}$) is a possible explanation, but it has no ability to predict the speed and direction of the Milky Way.

The hypothesis of absolute gravity has the power to predict this velocity. The Milky Way's velocity of 259 km/s is within 0.8 percent of its prediction of 261 km/s. The latitude of its direction (galactic: $l = 210° \pm 7,\ b = -2° \pm 6$; equatorial: $\alpha = 99.7°,\ \delta = 1.7°$) is just 1.7° above the gravitational plane, which is within 1.9 percent (1.7°/90°) of being parallel to it. The longitude of its direction is 21.7° from being perpendicular to Paradise ($\alpha = 168°$) in a counterclockwise direction. This is within 12.1 percent (21.7°/180°) of the prediction. Absolute gravity precisely predicts the speed of the Milky Way and its direction along the gravitational plane. It gives a reasonably accurate prediction of its counterclockwise direction of revolution, since distance measurements have a typical accuracy of about ± 10 percent.

The successful prediction of the velocity of the Milky Way is dynamic evidence of the action of absolute gravity. And its orbital velocity is consistent with a statement in the book. At 259 km/s and a radius of 9 Mly, Uversa completes one revolution around Paradise every 64.8 billion years. Our sun is "a few billion years past the swing around the southern curvature so that you are just now advancing beyond the southeastern bend." [15:1.5] From south to southeast is one-eighth of a revolution or 8.1 billion years. This can be fairly characterized as "a few billion years."

The Milky Way's velocity is calculated by assuming the redshift-distance relation is caused by a universal gravitational potential emanating from Paradise. Cosmological redshift is apparent out to the limits of observation, which can be explained by this gravitational potential. Absolute gravity causes this potential which pulls all galaxies toward Paradise, but they are not moving toward it. If they were approaching Paradise, their light would be blueshifted, instead of redshifted. Their ability to resist the pull of absolute gravity can be explained by their revolution around Paradise. Circular motion causes an inertial reaction equal and opposite to the action of gravity in a stable orbit.

12. The Expansion of Cosmic Consciousness

The explanation for the redshift-distance relation in the standard model relies on general relativity and numerous unverifiable assumptions concerning the original state of the universe, a big bang event, cosmic inflation, dark matter, dark energy, the cosmic microwave background, and the universal curvature of spacetime. (This last assumption became unverifiable in 2015 with the conclusive determination that the observable universe has no detectable spacetime curvature. [20] Any other finding would have contradicted the new model.) Cosmologists are repeatedly confronted by the need for new hypotheses to save the model from being refuted by the evidence. The latest theoretical crisis involves differing measurements of the Hubble constant that will likely require a new hypothesis. [23] The ever-increasing complexity of this theory is a clear indication to some scientists that it has failed. [24] [26] But there appears to be no alternative theory which gives a more credible explanation for the redshift-distance relation.

XXXVIII. The Field of Gravitational Potential in the Master Universe

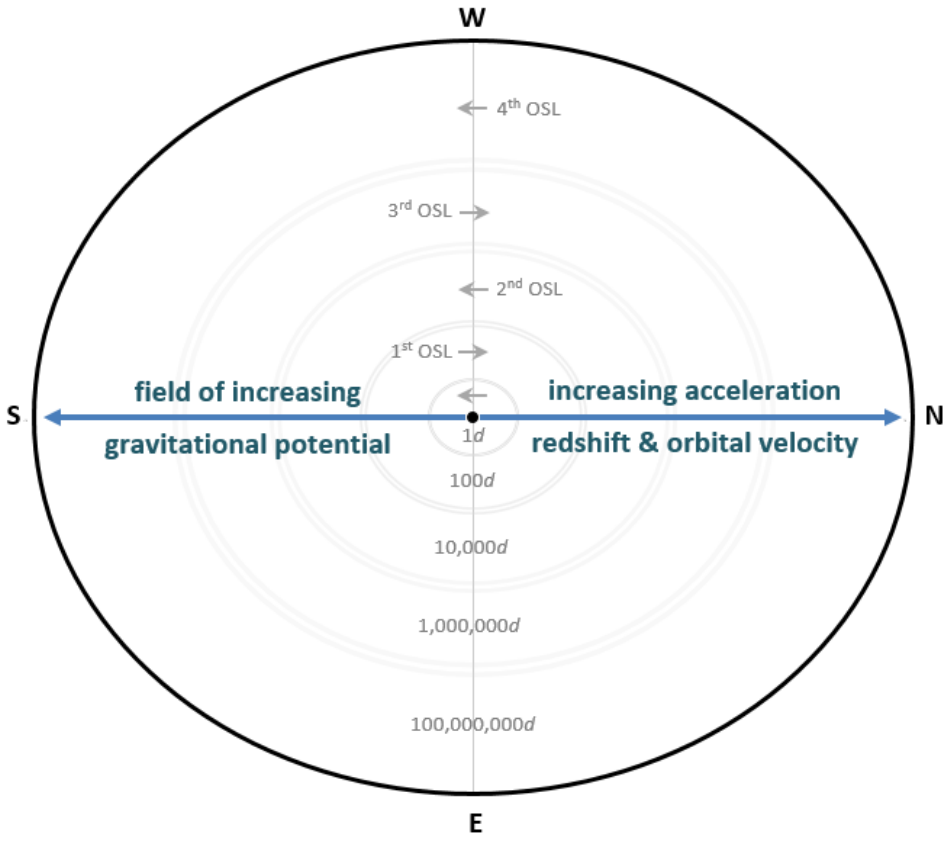

The Advent of *The Urantia Book* brings a new cosmological paradigm. Universal revolution is caused by the acceleration of absolute gravity acting from Paradise. The acceleration increases in direct proportion to the distance from Paradise. Redshift

increases in direct proportion to this acceleration. The universal redshift-distance relation is explained by the time dilation caused by the gravitational potential created by acceleration. This new model is explicable by the physics of special relativity. It requires no hypotheses, except for the unverifiable assumption that the Isle of Paradise is composed of a unique type of unobservable matter.

There is substantial evidence of the action of absolute gravity and the material reality of Paradise. The 2dF ring of galaxies, the Sloan Great Wall, and their planar alignment are evidence of the effects of absolute gravity. The redshift-distance relation is evidence of the universal field of gravitational potential created by absolute gravity. The Milky Way's velocity is evidence of the action of absolute gravity. The co-location of the universal center of revolution, the origin of gravitational potential, and the focus of gravitational attraction are evidence of the materiality of the Isle of Paradise.

The Urantia Book expands cosmic consciousness. It enlarges physical understanding which begins to be philosophically commensurate with the vision of a potentially infinite universe revolving around the First Source and Center. 0:3.13, 111:6.6 This new vision rests upon the postulate of an infinite inertial frame 105:3.4 centered on Paradise, 104:4.26-28 which is composed of an absolutely unique form of materialization. 11:2.9 105:7.2 This eternal inertial frame 118:4.3 is the metaphysical foundation for the temporal inertial frames of relativistic physics, which replaced classical inertial frames of absolute space. Conceptually, this is the third postulate of special relativity, since it associates temporal inertial frames with the eternal inertial frame established by Paradise and the Unqualified Absolute. 105:3.4

This third postulate is consistent with the statements, "the absolute of time is eternity," 12:5.2 and "a cycle of eternity [is] in some way synchronized with the transient material cycles of time." 32:5.4 The cycles of eternity are the absolute measure of the cycles of time, and a Paradise cycle has a period of two billion years. 13:3.2 The action of absolute gravity in this eternal inertial frame supersedes the action of linear gravity on large cosmic scales. 56:1.2 "Motion and universe gravitation are twin facets of the impersonal time-space mechanism of the universe of universes." 42:11.4 Absolute motion and gravity occur relative to Paradise, which controls the material universe. 1:2.10 The transcendence of time and space by the instantaneous action-at-a-distance exhibited by absolute gravity 107:6.4 and quantum entanglement [22] is evidence of transcendental causation 105:7.1 occurring on ultimate levels of reality. 0:1.12

Beauty consists in the harmony of unity, [2:7.8] and there is a beautiful cosmic symmetry in the fact that radial harmonic motion describes both the revolving universe and quantum phenomena, the very largest and smallest of material realities. [104.4.9] Machiventa Melchizedek, who co-authors the paper on Universal Unity, tells us that cosmology is the pursuit of beauty, and "supreme beauty… [is] …the unification of the cosmic extremes of Creator and creature." [56:10.3] "… thus even cosmology leads to the pursuit of divine reality values – to God-consciousness." [56:10.8]

References

[1] **The Realm of the Nebulae**, Edwin Hubble, 1958 (reprint of 1936 edition), Dover Publications, SBN 486-60455-1
https://archive.org/details/TheRealmOfTheNebulae

[2] **The SAO Encyclopedia of Astronomy** website
http://astronomy.swin.edu.au/cosmos/L/Local+Group

[3] **Redshifts and Magnitudes of Extragalactic Nebulae**, M. L. Humason et al., April 1956, *The Astrophysical Journal* [ads ref. code: 1956AJ.....61...97H]
A complete list of these 812 galaxies from NASA's Extragalactic Database at:
https://ned.ipac.caltech.edu/cgi-bin/objsearch?search_type=Search&refcode=1956AJ.....61...97H

[4] **NASA Extragalactic Database** website
https://ned.ipac.caltech.edu/

[5] **Sloan Digital Sky Survey** website
https://www.sdss.org/dr12/scope/

[6] **A Map of the Universe**, J. Richard Gott, et al., 2003 (preprint), published 2005 in *The Astrophysical Journal*, Volume 624, Number 2
https://arxiv.org/abs/astro-ph/0310571

[7] **Super-Large-Scale Structures in the Sloan Digital Sky Survey**, Deng, Xin-Fa, et al., Feb. 2006, *Chinese Journal of Astronomy and Astrophysics*, Volume 6, Issue 1
https://iopscience.iop.org/article/10.1088/1009-9271/6/1/004

[8] **The Mathematical Principles of Natural Philosophy**, Issac Newton, 1687; 1846 Edition of 1729 English translation by Andrew Motte, published in by Daniel Adee, New York, Book I, Proposition XI, pp. 116-117
https://openlibrary.org/books/OL7089085M/Newton's_Principia

[9] *ibid*. Book I, Proposition X, pp. 114-115

[10] **Theorem Relating to the Movement of a Point Attracted to a Fixed Center**, Joseph Bertrand, 1873; English translation of Bertrand's theorem, F. C. Santos, et al., April 2007
https://arxiv.org/abs/0704.2396

[11] **Never at Rest: A Biography of Isaac Newton**, Richard S. Westfall, 1980, Cambridge University Press, ISBN 978-0-521-27435-7, pp. 440-441

> "[Newton] recognized the privileged status of two force laws: forces that decrease in proportion to the distance squared, and forces that increase in proportion to the distance…. Among physically probable laws of attraction, only these two laws yield orbits whose lines of apsides do not move. When he studied the problem of many bodies attracting each other, he did so in terms of the two forces. He found that the presence of any number of bodies, all attracting by forces that increase in proportion to distance, does not disturb the perfect ellipticity of orbits and the proportionality of areas described to time, although it does increase the velocities and decrease the periods. As we have seen, the same does not hold for the inverse-square law. In that case, a third body always destroys perfect ellipticity…"

[12] **How I Created the Theory of Relativity,** Albert Einstein, Dec 14, 1922, translation by Yoshimasa A. Ono appearing in *Physics Today,* August 1982
https://www.jstor.org/stable/27757844?seq=1#page_scan_tab_contents

[13] **Einstein's Comprehensive 1907 Essay on Relativity**, English translation by H. M. Schwartz, June, Sep, Oct 1977, *American Journal of Physics,* Vol 45, No. 6, 9, 10 (Part III)
http://hermes.ffn.ub.es/luisnavarro/nuevo_maletin/Einstein_1907_Jahrbuch.pdf

[14] **The Gravitational Redshift**, R. F. Evans, J. Dunning-Davies, March 2004
https://arxiv.org/abs/gr-qc/0403082

[15] **Relativity in the Global Positioning System**, Neil Ashby, 2003, Living Reviews in Relativity, Volume 6, Issue 1, second term in equation (35)
https://link.springer.com/article/10.12942%2Flrr-2003-1

[16] **Our Peculiar Motion Away from the Local Void**, R. Brent Tully, Dec 2007, *Astrophysical Journal*
https://arxiv.org/abs/0705.4139

[17] *ibid*., pg. 12

[18] *ibid*., pg. 15

[19] *ibid*., pg. 14

[20] **Planck 2015 results. XIII. Cosmological Parameters**, Planck Collaboration Team, Feb 5 2015, pg. 39
https://arxiv.org/abs/1502.01589

[21] **Tests for the Expansion of the Universe**, Martin Lopez-Corredoira, July 2014, *Frontiers of Fundamental Physics* 14
https://arxiv.org/abs/1501.01487

[22] **Cosmic Bell Test Using Random Measurement Settings from High-Redshift Quasars**, Dominik Rauch, et al., Aug 20 2018, *Physical Review Letters,* 121, 080403
https://journals.aps.org/prl/abstract/10.1103/PhysRevLett.121.080403

[23] **Debate over the universe's expansion rate may unravel physics**, Jul 30 2019, *Science News*
https://www.sciencenews.org/article/debate-universe-expansion-rate-hubble-constant-physics-crisis

[24] **Cosmology Has Some Big Problems**, Apr 30 2019, *Scientific American*,
"Newton's physical laws made up a theoretical framework that worked for our own solar system…. But as the scales grew larger, its validity proved limited. Einstein's general relativity framework provided an extended and more precise reach beyond the furthest reaches of our own galaxy. But just how far could it go? …. It is, of course, entirely plausible that the validity of general relativity breaks down much closer to our own home than at the edge of the hypothetical end of the universe. And if that were the case, today's multilayered theoretical edifice of the big bang paradigm would turn out to be a confusing mix of fictional beasts invented to uphold the model, along with empirically valid variables mutually reliant on each other to the point of making it impossible to sort science from fiction."
https://blogs.scientificamerican.com/observations/cosmology-has-some-big-problems/

[25] **The 200-Inch Telescope and Some Problems It May Solve**, Edwin Hubble, 1947, *Publications of the Astronomical Society of the Pacific,* Vol. 59, No. 349, pg. 166

> "Attempts have been made to attain the necessary precision with the 100-inch, and the results appear to be significant. If they are valid, it seems likely that redshifts may not be due to an expanding universe…"
> http://adsabs.harvard.edu/full/1947PASP...59..153H

[26] **POP Goes the Universe**, Anna Ijjas, Paul J. Steinhardt and Abraham Loeb, Jan 2017, *Scientific American*

> "A common misconception is that experiments can be used to falsify a theory. In practice, a failing theory gets increasingly immunized against experiment by attempts to patch it. The theory becomes more highly tuned and arcane to fit new observations until it reaches a state where its explanatory power diminishes to the point that it is no longer pursued. The explanatory power of a theory is measured by the set of possibilities it excludes. More immunization means less exclusion and less power."
> http://physics.princeton.edu/~steinh/Ijjas-1P-120616.pdf

APPENDIX – The Local Group Galaxies in Orvonton

The Local Group of galaxies was identified by Edwin Hubble in his 1936 work *The Realm of the Nebulae.* It consisted of 9 galaxies: the Milky Way, LMC, SMC, Andromeda, Messier 32, NGC 205, Triangulum, NGC 6822, and IC 1613. The number of definite member galaxies in this group is now 99, as shown in Table 1. Over 60 percent of these have been discovered since 2000. There are 5 possible member galaxies which may also be gravitationally bound to the Local Group for a total of 104 galaxies. All 104 galaxies fit within a 51.4° wedge whose apex is 9.2 Mly distant from the Milky Way, as shown in Chart 1.

The Milky Way has a current total of 52 satellite galaxies. Andromeda has a current total of 32 satellites. There are 13 other galaxies which are not satellites of either. The 99 definite members of the LG are contained within an ellipsoidal volume of 105 million light-years cubed (Mly^3) (see calculation following Chart 3). This gives a galactic density of 0.94 gal/Mly^3 in the LG. The radius for a spherical volume of 105 Mly^3 is 2.9 Mly. Astronomers estimate the radius of the LG is about 3.3 Mly.

This high galactic density in the LG cannot be projected out to the central core in the 2dF ring of galaxies, which extends about 4 Mly to either side of the kernel. Most of the LG galaxies are too faint to be seen at these much greater distances. Only 43 LG members have an intrinsic luminosity that is bright enough (absolute magnitude $\boldsymbol{M} \leq -9$) to be observable by the 2dF Galaxy Redshift Survey telescope. This lower number of galaxies leads to an expected density of 0.41 gal/Mly^3 for 2dF galaxies in the central core of the superuniverse space level. The observed density in the central core of 0.64 gal/Mly^3 is comparable.

Table 1: Local Group Galaxies

Updated through June 2019

	Name	*R.A.* (1)	*Dec.* (2)	*kpc* (3)	*Mly* (4)	*Disc.* (5)	*Mbr* (6)	*m* (7)	*M* (8)
1	Milky Way	266.40	-28.94	8	0.03	prehist	LG		-20.9
2	Canis Major Dwarf	108.15	-27.67	8	0.03	2003 [1]	MW	-0.1	-14.6
3	Draco II	238.15	64.56	20	0.07	2015 [2]	MW	13.6	-2.9
4	Columba I	82.86	-28.03	25	0.08	2015 [5]	MW	12.5	-4.5
5	Sagittarius dSph	283.83	-30.55	27	0.09	1994 [6]	MW	3.6	-13.9
6	Hydrus I	37.39	-79.31	28	0.09	2018 [4]	MW	12.5	-4.7
7	Carina III	114.63	-57.90	28	0.09	2018 [7]	MW	14.8	-2.4
8	Triangulum II	33.32	36.18	30	0.10	2015 [8]	MW	15.6	-1.8
9	Ursa Major II	132.88	63.13	34	0.11	2006 [9]	MW	13.3	-4.3
10	Segue 2	34.82	20.18	36	0.12	2009 [10]	MW	15.2	-2.6
11	Carina II	114.11	-58.00	36	0.12	2018 [7]	MW	13.3	-4.5
12	Willman 1	162.34	51.05	41	0.13	2004 [11]	MW	15.2	-2.9
13	Coma Dwarf	186.75	23.90	44	0.14	2006 [3]	MW	14.1	-4.1
14	Tucana V	354.35	-63.27	44	0.14	2015 [5]	MW	16.6	-1.6
15	Bootes II	209.50	12.85	49	0.16	2007 [12]	MW	15.4	-3.0
16	LMC	80.89	-69.76	50	0.16	prehist	MW	0.1	-18.3
17	Tucana III	359.15	-59.60	55	0.18	2015 [5]	MW	16.3	-2.4
18	SMC	13.19	-72.83	61	0.20	prehist	MW	1.9	-17.0
19	Bootes I	210.05	14.49	62	0.20	2006 [13]	MW	12.8	-6.2
20	Tucana II	342.98	-58.57	63	0.21	2015 [14]	MW	15.2	-3.8
21	Sagittarius II	298.16	-22.10	67	0.22	2015 [2]	MW	13.9	-5.2
22	Leavens 3	316.75	14.97	67	0.22	2015 [2]	MW	14.7	-4.4
23	Ursa Minor Dwarf	227.29	67.22	72	0.23	1955 [16]	MW	10.6	-8.7
24	Horologium II	49.13	-54.14	79	0.26	2015 [15]	MW	16.9	-2.6
25	Draco Dwarf	260.05	57.92	81	0.26	1955 [16]	MW	10.6	-8.9
26	Sculptor Dwarf Elliptical	15.04	-33.71	82	0.27	1938 [17]	MW	8.6	-11.0
27	Sextans Dwarf Spheroidal	153.26	-1.61	85	0.28	1990 [18]	MW	10.4	-9.2

	Name	*R.A.* (1)	*Dec.* (2)	*kpc* (3)	*Mly* (4)	*Disc.* (5)	*Mbr* (6)	*m* (7)	*M* (8)
28	Phoenix II	355.00	-54.41	89	0.29	2015 [14]	MW	16.8	-2.8
29	Virgo I	180.04	-0.68	91	0.30	2016 [58]	MW	19.0	-0.8
30	Reticulum III	56.36	-60.45	92	0.30	2015 [5]	MW	16.5	-3.3
31	Ursa Major I Dwarf	158.72	51.92	101	0.33	2005 [20]	MW	14.4	-5.6
32	Carina Dwarf Spheroidal	100.40	-50.97	104	0.34	1977 [21]	MW	11.0	-9.1
33	Aquarius II	338.48	-9.33	110	0.36	2016 [22]	MW	15.8	-4.4
34	Crater II Dwarf	177.31	-18.41	118	0.38	2016 [23]	MW	12.2	-8.2
35	Grus I	344.18	-50.16	120	0.39	2015 [14]	MW	17.0	-3.4
36	Antlia II	143.89	-36.77	132	0.43	2018 [24]	MW	11.6	-9.0
37	Hercules Dwarf	247.76	12.79	136	0.44	2006 [3]	MW	14.0	-6.7
38	Fornax Dwarf Spheroidal	40.00	-34.45	140	0.46	1938 [25]	MW	7.4	-13.3
39	Hydra II	185.43	-31.99	142	0.46	2015 [26]	MW	16.0	-4.8
40	CVn II dSph	194.29	34.32	153	0.50	2006 [3]	MW	16.1	-4.8
41	Leo IV	173.24	-0.53	157	0.51	2007 [3]	MW	15.1	-5.9
42	Leo V	172.79	2.22	182	0.59	2008 [27]	MW	16.0	-5.3
43	Pisces II	344.63	5.95	182	0.59	2010 [28]	MW	16.3	-5.0
44	Grus II	331.02	-46.44	182	0.59	2015 [5]	MW	17.4	-3.9
45	Pegasus III Dwarf	336.09	5.42	205	0.67	2015 [29]	MW	17.5	-4.1
46	Bootes IV	233.69	43.73	209	0.68	2019 [61]	MW	17.1	-4.5
47	Tucana IV	0.73	-60.85	214	0.70	2015 [5]	MW	18.2	-3.5
48	CVn I dSph	202.01	33.56	216	0.70	2006 [31]	MW	13.8	-7.9
49	Leo II	168.37	22.15	219	0.71	1950 [30]	MW	12.0	-9.7
50	Leo I	152.12	12.31	245	0.80	1950 [30]	MW	10.1	-11.8
51	Cetus III	31.33	-4.27	251	0.82	2017 [19]	MW	19.6	-2.4
52	Eridanus II	56.09	-43.53	359	1.17	2015 [14]	MW	16.2	-6.6
53	Leo T	143.72	17.05	412	1.34	2007 [32]	MW	15.1	-8.0
54	Phoenix Dwarf	27.78	-44.44	418	1.36	1977 [33]	LG	12.0	-11.1
55	NGC 6822	296.24	14.80	480	1.56	1884	LG	8.1	-15.4
56	And XVI	14.87	32.38	555	1.81	2007 [34]	M31	14.4	-9.3

	Name	*R.A.* (1)	*Dec.* (2)	*kpc* (3)	*Mly* (4)	*Disc.* (5)	*Mbr* (6)	*m* (7)	*M* (8)
57	And II	19.12	33.42	649	2.12	1972 [35]	M31	11.7	-12.4
58	NGC 185	9.74	48.34	661	2.15	1787	M31	8.6	-15.7
59	And X	16.64	44.80	664	2.16	2006 [36]	M31	16.1	-8.0
60	And XXX	9.15	49.65	681	2.22	2012 [37]	M31	20.7	-3.44
61	NGC 147	8.30	48.51	725	2.36	1829	M31	8.9	-15.4
62	IC 1613	16.20	2.12	725	2.36	1906 [39]	LG	9.2	-15.1
63	AND IX	13.22	43.20	736	2.40	2004 [44]	M31	16.2	-8.2
64	IC 10	5.07	59.30	737	2.40	1887 [40]	LG	5.5	-19.3
65	Pisces Dwarf	15.98	21.89	737	2.40	1976 [41]	LG	14.3	-10.1
66	And III	8.89	36.50	744	2.43	1972 [35]	M31	14.4	-10.0
67	And XVII	9.28	44.32	748	2.44	2008 [38]	M31	15.8	-8.6
68	And XXIII	22.34	38.72	749	2.44	2011 [42]	M31	14.2	-10.2
69	And XXIV	19.63	46.37	749	2.44	2011 [42]	M31	16.3	-8.0
70	And XV	18.58	38.12	749	2.44	2007 [34]	M31	14.6	-9.8
71	And XXVIII	338.17	31.22	754	2.46	2011 [46]	M31	15.6	-8.8
72	And XXVI	5.94	47.92	758	2.47	2011 [42]	M31	17.3	-7.4
73	And XI	11.58	33.80	763	2.49	2006 [43]	M31	17.5	-6.9
74	And XIV	12.90	29.70	764	2.49	2007 [45]	M31	15.9	-8.5
75	Messier 32	10.67	40.87	768	2.50	1749	M31	7.1	-17.4
76	And XX	1.88	35.13	771	2.51	2008 [47]	M31	18.2	-6.2
77	Cassiopeia Dwarf	351.63	50.68	773	2.52	1999 60	M31	11.8	-12.9
78	And I	11.42	38.04	778	2.54	1972 [35]	M31	12.7	-11.8
79	And XXIX	359.73	30.76	780	2.54	2011 [50]	M31	16.0	-8.5
80	Andromeda Nebula	10.68	41.27	784	2.56	prehist	LG	2.7	-21.8
81	Cetus Dwarf Spheroidal	6.55	-11.04	789	2.57	1999 [49]	LG	13.2	-11.3
82	And XXV	7.54	46.85	791	2.58	2011 [42]	M31	14.8	-9.7
83	And V	17.57	47.63	795	2.59	1998 [51]	M31	15.3	-9.2
84	Leo III	149.86	30.75	800	2.61	1942 [52]	LG	12.4	-12.2
85	And XXVII	9.36	45.39	806	2.63	2011 [42]	M31	16.7	-7.8
86	And XXI	358.70	42.47	815	2.66	2009 [53]	M31	14.8	-9.8

	Name	*R.A.* (1)	*Dec.* (2)	*kpc* (3)	*Mly* (4)	*Disc.* (5)	*Mbr* (6)	*m* (7)	*M* (8)
87	NGC 205	10.09	41.69	821	2.68	1773	M31	8.0	-16.6
88	Peg dSph	357.94	24.58	841	2.74	1999 [48]	M31	13.2	-11.4
89	And XIII	12.96	33.00	841	2.74	2006 [43]	M31	18.1	-6.5
90	And XIX	4.88	35.04	852	2.78	2008 [47]	M31	15.6	-9.1
91	And XII	11.86	34.37	862	2.81	2006 [43]	M31	18.3	-6.4
92	Triangulum Galaxy	23.46	30.66	870	2.84	prehist	LG	5.28	-19.4
93	Tucana Dwarf	340.46	-64.42	886	2.89	1991 [54]	LG	15.2	-9.5
94	And XXII	21.92	28.09	904	2.95	2009 [53]	M31	18.0	-6.8
95	WLM	0.49	15.46	973	3.17	1909	LG	10.2	-14.8
96	Aquarius dIrr	311.72	-12.85	988	3.22	1959 [55]	LG	13.6	-11.3
97	Peg DIG	352.15	14.74	1009	3.29	1955 [16]	LG	11.32	-13.7
98	Sag DIG	292.50	-17.68	1072	3.49	1977 [59]	LG	13.6	-11.5
99	NGC 3109	150.78	26.16	1244	4.06	1835	LG?	9.5	-16.0
100	And XVIII	0.56	45.09	1302	4.24	2008 [47]	M31	16.0	-9.57
101	Antlia Dwarf	151.02	-27.33	1320	4.30	1985 [56]	LG?	14.14	-11.46
102	Sextans A	152.75	4.69	1363	4.44	1990 [18]	LG?	11.36	-14.31
103	Sextans B	150.00	5.33	1402	4.57	1990 [18]	LG?	11.05	-14.68
104	Leo P	155.44	18.09	1429	4.66	2013 [57]	LG?	15.72	-10.0

(1) **R.A.** Right ascension in equatorial coordinates (J2000)
(2) **Dec.** Declination in equatorial coordinates (J2000)
(3) **kpc** Distance in kiloparsecs
(4) **Mly** Distance in millions of light-years (Mly)
(5) **Disc.** Year discovered and documentation reference
(6) **Mbr** Member of Local Group (LG) or satellite of the Milky Way (MW) or Andromeda (M31)
(7) **m** Apparent visual magnitude
(8) **M** Absolute visual magnitude

Table 2: Papers Announcing Discovery of Particular Galaxies

No.	*Paper*	*Link*
1	**A dwarf galaxy remnant in Canis Major**, N. F. Martin, Nov 2003	https://arxiv.org/abs/astro-ph/0311010
2	**Sagittarius II, Draco II and Laevens 3**, Benjamin, P.M., Oct 2015	https://arxiv.org/abs/1507.07564
3	**Cats and Dogs, Hair and A Hero**, V. Belokurov, Aug 2006	https://arxiv.org/abs/astro-ph/0608448
4	**Snake in the Clouds**, Sergey E. Koposov, Apr 2018	https://arxiv.org/abs/1804.06430
5	**Eight Ultra-faint Galaxy Candidates**, DES Collaboration, Aug 2015	https://arxiv.org/abs/1508.03622
6	**A dwarf satellite galaxy in Sagittarius**, Ibata, R. A., Jul 1994	http://adsabs.harvard.edu/abs/1994Natur.370..194I
7	**Discovery of two neighboring satellites**, G. Torrealba, Jan 2018	https://arxiv.org/abs/1801.07279
8	**A New Faint Milky Way Satellite,** Benjamin P. M. Laevens, Mar 2015	https://arxiv.org/abs/1503.05554
9	**A Curious New Milky Way Satellite in Ursa Major,** D.B. Zucker, Jun 2006	https://arxiv.org/abs/astro-ph/0606633
10	**Segue 2,** V. Belokurov, Mar 2009	https://arxiv.org/abs/0903.0818
11	**A New Milky Way Companion**, Beth Willman, Oct 2004	https://arxiv.org/abs/astro-ph/0410416
12	**A Pair of Bootes**, S.M. Walsh, May 2007	https://arxiv.org/abs/0705.1378
13	**A Faint New Milky Way Satellite in Bootes**, V. Belokurov, Apr 2006	https://arxiv.org/abs/astro-ph/0604355
14	**Beasts of the Southern Wild**, Sergey E. Koposov, Mar 2015	https://arxiv.org/abs/1503.02079
15	**Horologium II**, Dongwon Kim, May 2015	https://arxiv.org/abs/1505.04948
16	**Sculptor-Type Systems in the Local Group**, A. G. Wilson, Feb 1955	http://adsabs.harvard.edu/abs/1955PASP...67...27W
17	**A Stellar System of a New Type,** Shapely, H., Mar 1938	https://www.nature.com/articles/142715b0
18	**A new satellite galaxy of the Milky Way**, Irwin, M. J., May 1990	http://adsabs.harvard.edu/abs/1990MNRAS.244P..16I
19	**Discovery of Cetus III**, Daisuke Homma, Apr 2017	https://arxiv.org/abs/1704.05977
20	**A New Milky Way Dwarf Galaxy in Ursa Major**, Beth Willman, May 2005	https://arxiv.org/abs/astro-ph/0503552
21	**A new Sculptor-type dwarf elliptical galaxy in Carina**, Cannon, R. D., Sep 1977	http://adsabs.harvard.edu/abs/1977MNRAS.180P..81C
22	**At the survey limits**, G. Torrealba, May 2016	https://arxiv.org/abs/1605.05338
23	**The feeble giant**, G. Torrealba, Jan 2016	https://arxiv.org/abs/1601.07178
24	**The hidden giant**, G. Torrealba, Nov 2018	https://arxiv.org/abs/1811.04082
25	**Two Stellar Systems of a New Kind**, Harlow Shapely, Oct 1938	http://adsabs.harvard.edu/abs/1938Natur.142..715S
26	**Hydra II**, Nicolas F. Martin, Mar 2015	https://arxiv.org/abs/1503.06216
27	**Leo V**, V. Belokurov, Jul 2008	https://arxiv.org/abs/0807.2831
28	**Big fish, small fish**, V. Belokurov, Feb 2010	https://arxiv.org/abs/1002.0504
29	**A Hero's Dark Horse**, Dongwon Kim, Mar 2015	https://arxiv.org/abs/1503.08268
30	**Two New Stellar Systems in Leo**, R. G. Harrington, 1950	http://adsabs.harvard.edu/full/1950PASP...62..118H
31	**A New Milky Way Dwarf Satellite in Canes Venatici**, D. B. Zucker, Apr 2006	https://arxiv.org/abs/astro-ph/0604354
32	**Discovery of an Unusual Dwarf Galaxy**, M.J. Irwin, Jan 2007	https://arxiv.org/abs/astro-ph/0701154
33	**A New Dwarf Irregular Galaxy**, R. Canterna, Oct 1976	http://adsabs.harvard.edu/full/1977ApJ...212L..57C
34	**The Haunted Halos of Andromeda and Triangulum**, R. Ibata, Apr 2007	https://arxiv.org/abs/0704.1318

Table 2: Papers Announcing Discovery of Particular Galaxies

No.	*Paper*	*Link*
35	**Search for Faint Companions to M31**, van den Bergh, Sidney, Jan 1972	http://adsabs.harvard.edu/abs/1972ApJ...171L..31V
36	**Andromeda X**, Daniel B. Zucker, Jan 2006	https://arxiv.org/abs/astro-ph/0601599
37	**Distances to the Satellites of M31**, Anthony R. Conn, Sep 2012	https://arxiv.org/abs/1209.4952
38	**Andromeda XVII**, Mike Irwin, Feb 2008	https://arxiv.org/abs/0802.0698
39	**Stellar Populations at the Center of IC 1613**, Andrew A. Cole, May 1999	https://arxiv.org/abs/astro-ph/9905350
40	**Catalogue No. 7 of Nebulae discovered at the Warner Observatory**, Swift, L., 1888	http://adsabs.harvard.edu/abs/1889AN....120...33S
41	**Distances and Metallicities for 17 Local Group Galaxies**, A.W. McConnachie, Oct 2004	https://arxiv.org/abs/astro-ph/0410489
42	**PAndAS' progeny**, Jenny C. Richardson, Feb 2011	https://arxiv.org/abs/1102.2902
43	**Discovery and analysis of three faint dwarf galaxies**, N. F. Martin, Jul 2006	https://arxiv.org/abs/astro-ph/0607472
44	**Andromeda IX**, Daniel B. Zucker, Apr 2004	https://arxiv.org/abs/astro-ph/0404268
45	**Discovery of Andromeda XIV**, Steven R. Majewski, Feb 2007	https://arxiv.org/abs/astro-ph/0702635
46	**Andromeda XXVIII**, Colin T. Slater, Oct 2011	https://arxiv.org/abs/1110.5903
47	**A trio of new Local Group galaxies**, Alan McConnachie, Jun 2008	https://arxiv.org/abs/0806.3988
48	**The Newly Discovered Dwarf Andromeda VI**, Taft E. Armandroff, May 1999	https://arxiv.org/abs/astro-ph/9905237
49	**A New Local Group Galaxy in Cetus**, Alan B. Whiting, Aug 1999	http://adsabs.harvard.edu/abs/1999AJ....118.2767W
50	**Andromeda XXIX**, Eric F. Bell, Oct 2011	https://arxiv.org/abs/1110.5906
51	**The Newly Discovered Dwarf Andromeda V**, Taft E. Armandroff, Jul 1998	https://arxiv.org/abs/astro-ph/9807232
52	**On the Large Scale Distribution of Matter in the Universe**, F. Zwicky, Apr 1942	http://adsabs.harvard.edu/abs/1942PhRv...61..489Z
53	**PAndAS' cubs**, Nicolas F. Martin, Sep 2009	https://arxiv.org/abs/0909.0399
54	**A New Member of the Local Group**, Russell J. Lavery, Sep 1991	http://adsabs.harvard.edu/abs/1992AJ....103...81L
55	**Updated Information on the Local Group**, Sidney van den Bergh, Jan 2000	https://arxiv.org/abs/astro-ph/0001040
56	**The Nearest Group of Galaxies**, Sidney van den Bergh, Apr 1999	https://arxiv.org/abs/astro-ph/9904425
57	**Discovery of the Nearby Gas-Rich Dwarf Galaxy Leo P**, Evan D. Skillman, May 2013	https://arxiv.org/abs/1305.0277
58	**A New Milky Way Satellite Discovered**, Daisuke Homma, Sep 2016	https://arxiv.org/abs/1609.04346
59	**Two new faint stellar systems discovered**, Cesarsky, D. A., Nov 1977	http://adsabs.harvard.edu/abs/1977A%26A....61L..31C
60	**HI observations of nearby galaxies**, I. D. Karachentsev, Nov 1999	https://arxiv.org/abs/astro-ph/9911350
61	**Bootes IV: A New Milky Way Satellite,** Daisuke Homma, Jun 2019	https://arxiv.org/abs/1906.07332

Chart 1: Polar View of the Local Group of Galaxies

Looking Down on Equatorial Plane (Plane of Creation)

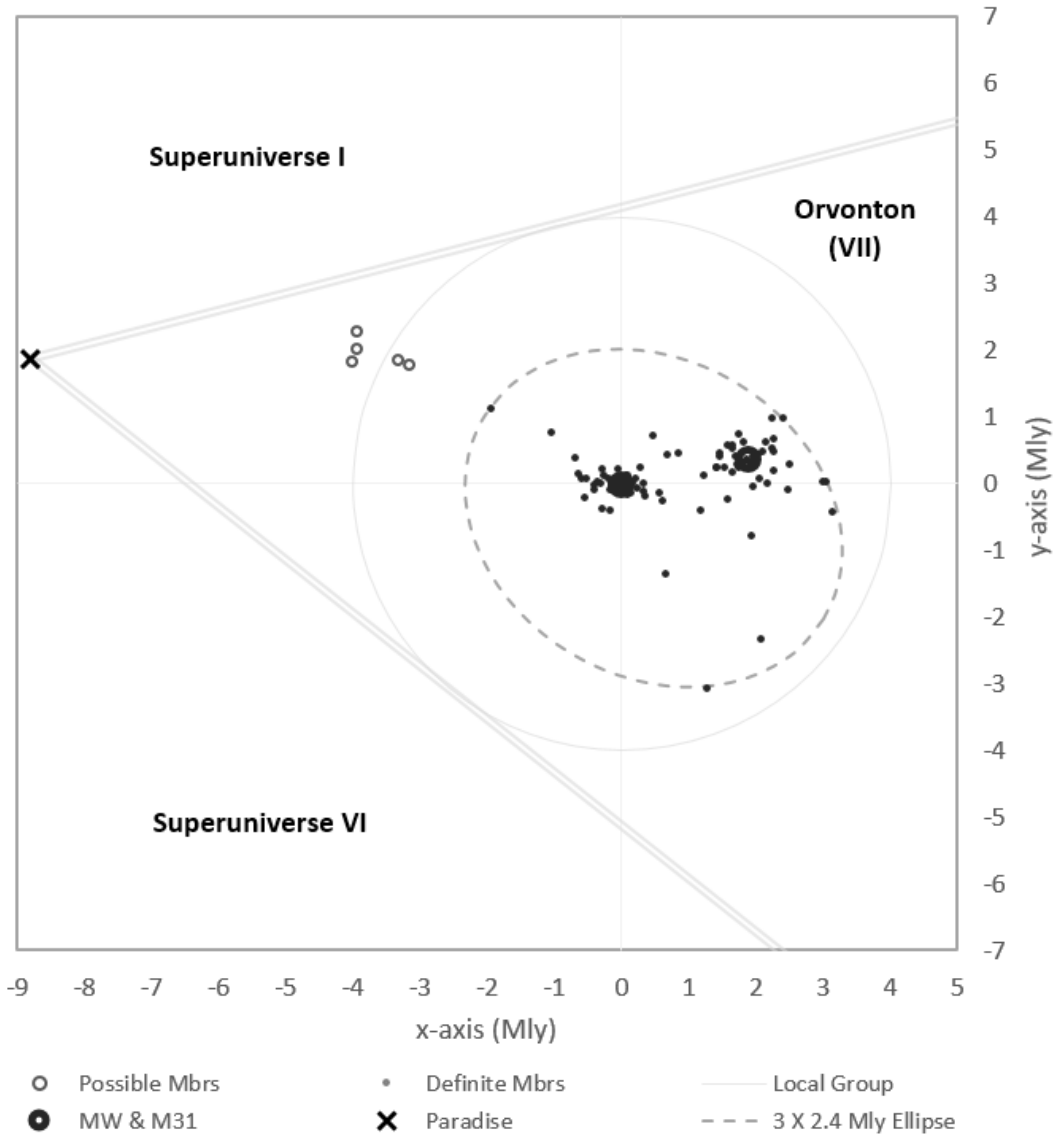

Definite members of Local Group are contained by an ellipse with a semi-major axis of 2.95 Mly and semi-minor axis of 2.38 Mly. Ellipse center $(-0.67, 0.20)$. Ellipse is rotated clockwise $31°$.

Chart 2: Side View of the Local Group of Galaxies

YZ Plane is set perpendicular to the MW-M31 axis

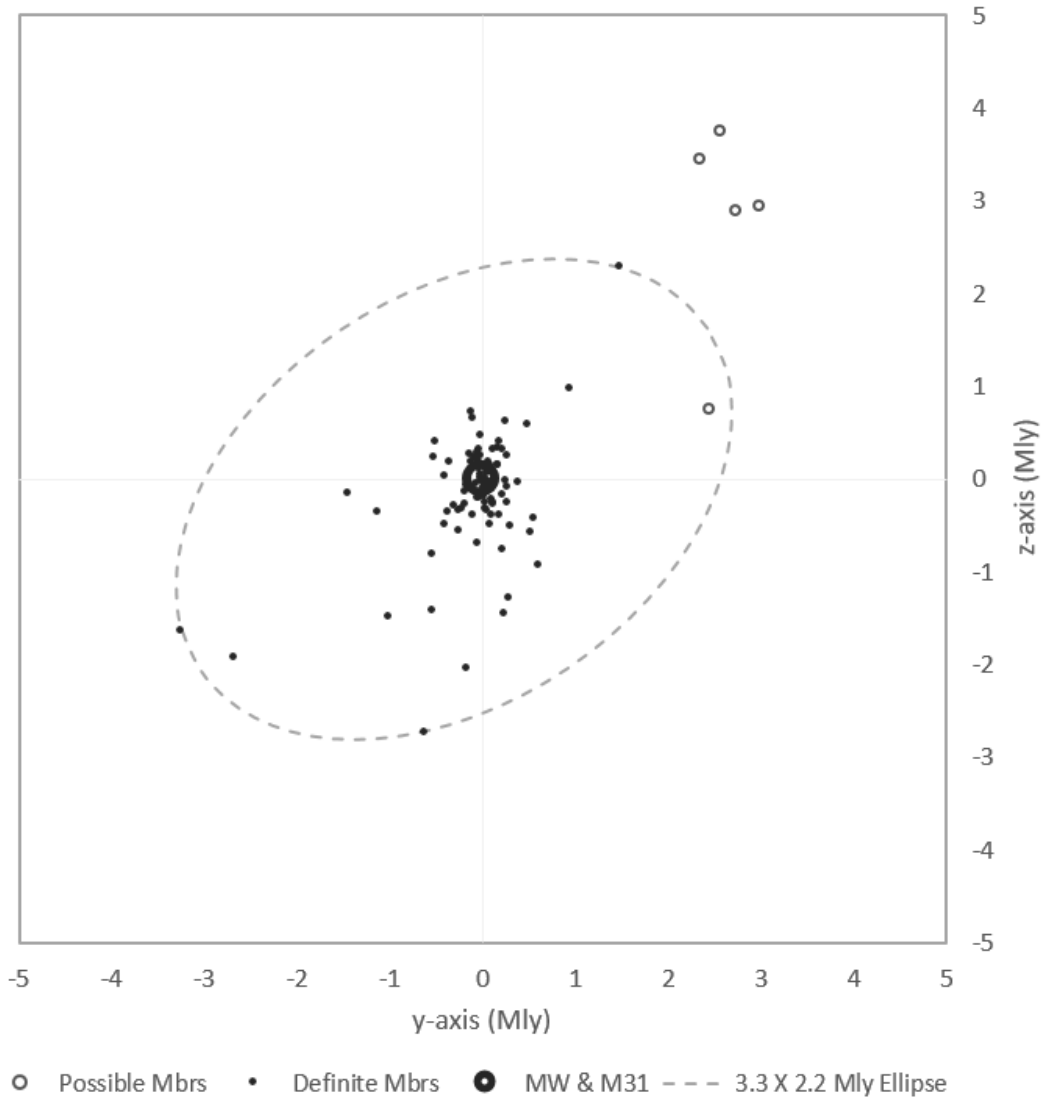

Cartesian coordinates of galaxies are rotated for Chart 2 and Chart 3. Coordinates in the XY plane are rotated counterclockwise $10.68°$ so that both the Milky Way (MW) and Andromeda (M31) are on the XZ plane. (Andromeda has an equatorial longitude of $\alpha = 10.68°$). Coordinates in the YZ plane are then rotated clockwise $41.77°$ so that both the Milky Way (MW) and Andromeda (M31) are on the x-axis (Andromeda has an equatorial latitude of $\delta = 41.77°$).

Definite members of Local Group are contained by an ellipse with a semi-major axis of 3.3 Mly and a semi-minor axis of 2.2 Mly. Ellipse center $(-0.38, 0.0)$. Ellipse is rotated counterclockwise $34°$.

Chart 3: Side View of the Local Group of Galaxies

XZ Plane is aligned with the MW-M31 axis

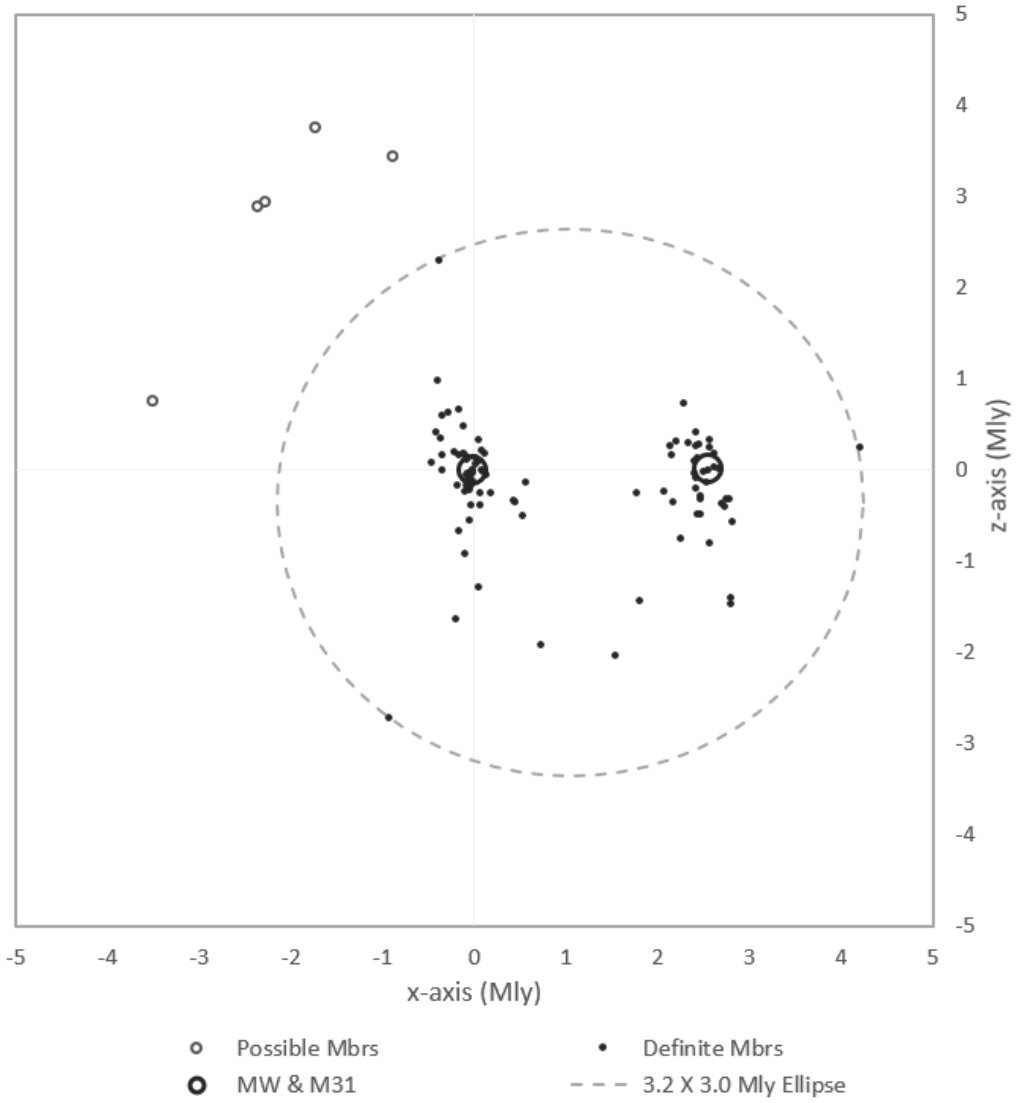

Definite members of Local Group are contained by an ellipse with a semi-major axis of 3.2 Mly and a semi-minor axis of 3.0 Mly. Ellipse center $(1.05, -0.35)$.

Volume of Ellipsoid containing Definite Members

XZ-plane: x-axis *a* = 3.2 Mly, z-axis *c* = 3.0 Mly (Chart 3)
YZ-plane: y-axis *b* = 3.3 Mly, z-axis *c* = 2.2 Mly (Chart 2)
a = 3.2, *b* = 3.3, *c* = 2.6 (avg. 3.0 & 2.2)

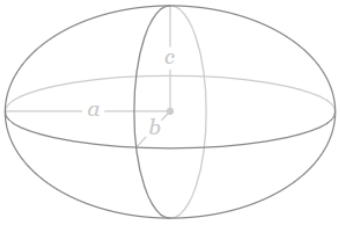

$$V = \frac{4}{3}\pi abc = 105\ Mly^3$$